Department of Forest Products Technology

Deformation and fracture mechanisms in nanocellulose reinforced composites

Mindaugas Bulota

A!

DOCTORAL DISSERTATIONS

Aalto University publication series
DOCTORAL DISSERTATIONS 109/2012

Deformation and fracture mechanisms in nanocellulose reinforced composites

Mindaugas Bulota

A doctoral dissertation completed for the degree of Doctor of Science (Technology) to be defended, with the permission of the Aalto University School of Chemical Technology, at a public examination held at the Auditorium Puu2 of the school on the 5th of October 2012 at 12 o'clock.

Aalto University
School of Chemical Technology
Department of Forest Products Technology

Supervising professor
Professor Mark Hughes, Aalto University, Finland

Preliminary examiners
Professor Wolfgang Gindl-Altmutter, University of Natural Resources and Life Sciences, Austria
Professor Kristiina Oksman, Luleå University of Technology, Sweden

Opponent
Professor Kristofer Gamstedt, Uppsala University, Sweden

Aalto University publication series
DOCTORAL DISSERTATIONS 109/2012

ISBN 978-952-60-4749-2 (printed)
ISBN 978-952-60-4750-8 (pdf)
ISSN-L 1799-4934
ISSN 1799-4934 (printed)
ISSN 1799-4942 (pdf)
http://urn.fi/URN:ISBN:978-952-60-4750-8

Unigrafia Oy
Helsinki 2012

Finland

441 697
Printed matter

Author
Mindaugas Bulota

Name of the doctoral dissertation
Deformation and fracture mechanisms in nanocellulose reinforced composites

Publisher School of Chemical Technology

Unit Department of Forest Products Technology

Series Aalto University publication series DOCTORAL DISSERTATIONS 109/2012

Field of research Wood Material Technology

Manuscript submitted 3 May 2012 **Date of the defence** 5 October 2012

Permission to publish granted (date) 19 June 2012 **Language** English

☐ **Monograph** ☒ **Article dissertation (summary + original articles)**

Abstract

Cellulose is the main constituent of plants. In the cell wall of plants, cellulose nanofibrils act as a reinforcing agent embedded in a matrix of hemicelluloses and lignin, forming a nanocomposite material. Manmade nanocellulose reinforced composites began to receive attention approximately two decades ago when isolation methods for nanocellulose were developed. However, studies on the deformation of these novel materials have been limited.

The effect of the composites' preparation method on the mechanical properties was investigated and compared with theoretical models. Deformation mechanisms in composites reinforced with low weight fractions of different types of nanocellulose were investigated along with the effects of acetylation. Then the stress-transfer and micromechanics of composites reinforced with higher weight fractions of nanocellulose were studied using Raman spectroscopy. Finally, the effect of nanocellulose on thermomechanical properties of the composites and their behaviour in moist environment were addressed.

The results show that the preparation method has an influence on the final mechanical properties of composites. Degassing of the nanocellulose/polymer mixture showed a positive effect on the Young's modulus and tensile strength at lower weight fractions of nanocellulose due to the lower viscosities of the mixtures. However, degassing had no effect on the density of the composites. Chemical modification significantly improved the dispersion of nanocellulose in non-polar media as Raman imaging revealed. In turn, the mechanical properties and deformation of the composites was different with respect to the degree of substitution. The toughening of poly(lactic) acid by the addition of low weight fractions of nanocellulose was attributed to extensive polymer crazing which was also dependent on the morphology and degree of substitution of the nanocellulose. Using Raman spectroscopy it was shown that the deformation micromechanics at high weight fractions of nanocellulose are network dominated. This leads to a stress transfer mechanisms similar to a composite within a composite, where composite strength is dependent on stress transfer within the dense network. The mechanical properties of the composites were improved as well as the glass transition temperature. The crystallization behaviour and, in turn, crystallinity of the composites was observed to be impeded at large weight fractions of nanocellulose. Furthermore, the composites had better mechanical properties in humid environments compared to the pure PLA matrix and the pure nanocellulose film. Thus embedding of hydrophilic fibrils in a hydrophobic matrix improves the performance of these materials in humid environments.

Keywords Nanocellulose, Micromechanics, Deformation, Composites

ISBN (printed) 978-952-60-4749-2 **ISBN (pdf)** 978-952-60-4750-8

ISSN-L 1799-4934 **ISSN (printed)** 1799-4934 **ISSN (pdf)** 1799-4942

Location of publisher Espoo **Location of printing** Helsinki **Year** 2012

Pages 131 **urn** http://urn.fi/URN:ISBN:978-952-60-4750-8

Preface

The study was carried out at the Department of Forest Products Technology at Aalto University. It commenced in January 2009 as a three-year project financed by the Academy of Finland. The experimental work was mainly accomplished at Aalto University within 3 years (2009-2011). A short term scientific mission was completed at the University of Manchester in spring 2011 in cooperation with Prof. Stephen Eichhorn and doctoral student (at that time) Supachok Tanpichai. It was partially financed by COST action FP0802. The last year of the doctoral studies was partially financed from the doctoral programme in the built environment (RYM-TO).

I'd like to express my gratitude to my supervisor Professor Mark Hughes who believed in me and gave an opportunity to work in this new emerging field. There were many people on my way towards the doctoral degree thus it is impossible to mention all of them. Nevertheless, I'd like to thank D.Sc. Tuomas Hänninen for introducing cellulose chemistry and Raman spectroscopy to me. Many thanks go to the people in Puu1, in particular, Anna Olszewska and Dr. Michael Hummel for valuable discussions regarding chemistry and not only that. I'm grateful to Kätlin Kreitsmann who carried out a large amount of experimental work during her Master's thesis studies at the Department of Forest Products Technology. Furthermore, I cordially thank Professor Stephen Eichhorn for introducing polymer crazing to me as well as sharing his valuable opinions as well as Supachok Tanpichai who taught me a lot about Raman Spectroscopy.

Special thanks are due to all teachers and colleagues at the Department of Forest Products Technology: Lauri R., Kristiina, Pekka, Anti, Toni, Olli, Arto, Atsushi, Jussi R., Lauri L., Katja, Pia, Tiina, Annika, Jaakko, Jonna, Jussi L., Mikko, Michael, Kimmo, Albert and all others whom I had a pleasure to work and study with.

Finally, I thank my family and friends who still remember me after being abroad for 6 years.

Espoo, 2012

List of publications

Paper I M.Bulota, A. S. Jääskeläinen, J. Paltakari, M.Hughes. 2011. Properties of biocomposites: influence of preparation method, testing environment and a comparison with theoretical models. Journal of Materials Science 46 (10) p. 3387. DOI 10.1007/s10853-010-5227-4

Paper II M. Bulota, K. Kreitsmann, M. Hughes, J. Paltakari. 2011. Acetylated microfibrillated cellulose (MFC) as toughening agent in poly(lactic) acid (PLA). Journal of Applied Polymer Science 126 (S1) pp E449-E458. DOI 10.1002/app.36787

Paper III M. Bulota, M. Hughes. 2012. Toughening mechanisms in poly(lactic) acid reinforced with TEMPO-oxidized cellulose. Journal of Materials Science 47 (14) p. 5517. DOI: 10.1007/s10853-012-6443-x

Paper IV M. Bulota, S. Tanpichai, M. Hughes, S. J. Eichhorn. 2011. Micromechanics of TEMPO-oxidized fibrillated cellulose composites. ACS Applied Materials & Interfaces 4 (1), pp 331–337. DOI: 10.1021/am201399q.

Paper V M. Bulota, A.H. Vesterinen, M. Hughes, J. Seppälä. 2012. Mechanical behaviour, structure and reinforcement processes of TEMPO-oxidized cellulose reinforced PLA. Submitted.

Author's contribution to the papers:

I Mindaugas Bulota was responsible for the research plan, experimental design, preparation and characterization of the composites films, performing all of the tests and SEM images, analysis of the data and preparation of the first version of the manuscript.

II-III Mindaugas Bulota was responsible for the research plan, experimental design, cellulose chemical modification, characterization, Raman and SEM imaging, data analysis and preparation of the first version of the manuscript.

IV Mindaugas Bulota was responsible for the research plan, experimental design, chemical modification, characterization and preparation of the composites films, SEM imaging. Some part of the Raman spectroscopy, data analysis and preparation of the first version of the manuscript.

V Mindaugas Bulota was responsible for the research plan, experimental design, chemical modification, characterization and preparation the composites films, data analysis and preparation of the first version of the manuscript.

List of Abbreviations

AA – Acetic anhydride

AFM – Atomic force microscopy

BC – Bacterial cellulose

CNC – Cellulose nanocrystals

DMTA – Dynamic mechanical thermal analysis

DS – Degree of substitution

DSC – Differential scanning calorimetry

FT-IR – Fourier transform infrared spectroscopy

MCC – Microcrystalline cellulose

MFC – Microfibrillated cellulose

NFC – Nanofibrillated cellulose

NC – Nanocellulose

PLA – Poly(lactic) acid

PVA – Poly(vinyl) alcohol

SEM – Scanning electron microscopy

TEMPO - 2,2,6,6-tetramethylpiperidine-1-oxyl radical

T_g – Glass transition temperature

T_m – Melting temperature

TEA – Tensile energy absorbed [J/m^2]

TOFC – TEMPO-oxidized fibrillated cellulose

XRD – X-ray diffraction

Table of Contents

1 INTRODUCTION AND OUTLINE OF THE STUDY

As the world population is gradually increasing there is a need to tackle ecological problems resulting from our enormous energy consumption and growing amount of wastes.

The production of plastics has been rising, by on average 9 %, annually since 1950 and in 2009 reached 230 million tonnes worldwide (Fig. 1). The greatest share of plastics is used in packaging (40 %) followed by the construction and building industry which accounts for 20 % of annual consumption (PEMRG Plastics Europe market research group 2010).

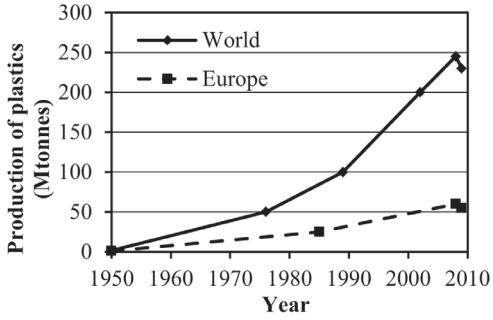

Figure 1. World and Europe plastics production 1950 – 2009 (PEMRG Plastics Europe market research group 2010).

The raw material for most plastics is crude oil and accounts for 4 - 5 % of total crude oil consumption and other 4 - 5 % is converted into energy for their production (Stevens 2001). In addition, the degradation time of synthetic petroleum-based plastics may be several hundred years, which can result in ecological disasters such as the “Great Pacific Garbage Patch” which is made up mainly of plastic junk and which is twice the size of the United States and is floating in the Pacific Ocean (Fig. 2).

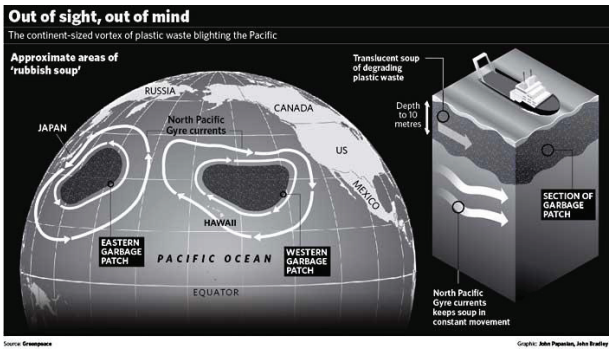

Figure 2. The Great Pacific Garbage Patch (Marks and Howden 2008). *Reprinted with permission from The Independent.*

This problem can be tackled through the greater use of renewable bio-based materials in everyday life. Humankind has been learning from nature and mimicking it for thousands of years, mostly intuitively. Wood is probably the most abundant natural material that has been used for thousands of years commercially. It is a nanocomposite where cellulose fibrils are embedded in a matrix of hemicelluloses and lignin. These fibrils, when isolated from the macrostructure of plants, are referred to as micro or nanocellulose (NC) depending on the width of fibrils. Furthermore, based on the aspect ratio and disintegration method, NC can be grouped into: microcrystalline cellulose (MCC), microfibrillated cellulose (MFC) and nanofibrillated cellulose (NFC) (Moon et al. 2011). Nevertheless, the categories are not strictly defined as the scientific community is still striving for standardization of nanocellulosic materials. Moreover, the morphology of nanocellulose is source dependant.

Nanocellulose is an attractive reinforcing agent due to its abundance throughout the world, inherent sustainability, carbon neutrality as well as its excellent thermal stability, high stiffness and low density (~ 1.5 g/cm^3). The first, cellulose (tunicate) reinforced polymer composites, however, were prepared only in 1995 by Favier and co-workers (Favier et al. 1995). This study started a new era of nanocellulose reinforced composite research.

It would be possible to decrease the annual production of plastics by 23 million tonnes only through the incorporation of 10 wt% of nanocellulose. This would lead to a substantial decrease in landfilling, which, for example, in the US was around 30 million tonnes (EPA - US Environmental Protection Agency 2010) and in Europe 24.3 million tonnes in 2009 (PEMRG Plastics Europe market research group 2010). Moreover a mixture of biopolymers with cellulose would provide compostable and potentially sustainable materials. Biopolymers, however, cannot compete with conventional synthetic petroleum-based plastics in terms of mechanical properties and price. Thus further studies are needed in order to design competitive bio-based materials.

Any material in its service life has to withstand mechanical loads, thus studies on its deformation mechanisms are very important. Since the nanocellulose reinforced composites research field is relatively new, the deformation and fracture mechanisms of these new materials are not yet well understood. Moreover various chemical treatments may be applied to nanocellulose in order to alter its properties which, in turn, affect mechanical behaviour. Due to recent developments in research tools it is possible to study deformation and fracture mechanisms in nanocomposites and contribute to the further development of these materials. Knowledge of the deformation mechanisms in these materials would also facilitate the tailoring of properties specific for ones needs and creating materials with unique properties which have never been achieved before.

The main objectives of this study were to investigate deformation and fracture mechanisms in nanocellulose reinforced composites. A number of ways such as extrusion, compression moulding or casting, just to name a few, can be used for the preparation of composites. A casting technique is a good way to prepare thin composite films having a thickness of ~ 50 – 100 μm which are suitable for studies on the structure and deformation mechanisms. Since casting methods can vary a lot amongst themselves, firstly, a study on the effect of the preparation method on the

mechanical properties of composites was carried out (**Paper I**). Based on the literature, the most often varied factors in the preparation of cast films are: concentration of the polymer solution, degassing of the cast and the mixing time of the dispersion. Thus the aforementioned were addressed in this study. A water-based synthetic biodegradable polymer - poly(vinyl) alcohol (PVA) was used as the matrix in **Paper I** due to its compatibility with cellulose. Thus the need for chemical modification was eliminated. The preparation process of the composites in **Paper II-V** was designed with respect to the findings in **Paper I**. Poly(lactic) acid was chosen as a matrix for further investigation since it is a bio-based and commercially available polymer. Esterification (acetylation) was carried out in order to hydrophobise the surface of NC and improve cellulose dispersion in low-polarity solvents. It was used in conjunction with two types of cellulose: microfibrillated cellulose (MFC) and 2,2,6,6-tetramethylpiperidine-1-oxyl radical (TEMPO)-oxidized fibrillated cellulose (TOFC). The effect of chemical modification (acetylation) on the structural organization of the composites and the deformation of composites was studied for MFC (**Paper II**) and TOFC (**Paper III**) reinforced PLA. Furthermore, the micromechanics, in particular the stress transfer from the matrix to cellulose nanofibrils, in composites with high weight fractions (> 15 wt%) of TOFC were studied using Raman spectroscopy (**Paper IV**). Finally the influence of high weight fractions of TOFC on the structure, crystallization and reinforcement processes in PLA composites was studied (**Paper V**).

2 BACKGROUND

2.1 Composite materials and cellulose

Most of the materials in nature are nanocomposites themselves, e.g. wood, teeth, bones, tendons, nacre (Abalone shell) and many more (Meyers et al. 2008). Over the course of millions of years nature itself has developed biological composite materials which are adapted to their environment. Plant-based nanocomposites have evolved by manipulating three main polymers: cellulose, hemicelluloses and lignin. The function of cellulose in these natural nanocomposites is that of reinforcement, with hemicelluloses and lignin acting as the matrix (O'Sullivan 1997). Cellulose can additionally be of animal (tunicate) or bacterial origin. The advantages of composite materials were already recognized in ancient Egypt as clay was reinforced with wheat straw and was used as a construction material. The first man made composite material based on fibrillated cellulose – paper, was invented around 100 BC in China. Surprisingly, since then there have been no landmark developments in the use of cellulosic fibres until the appearance of a paper by Turbak and co-workers in 1983 (Turbak et al. 1983) where microfibrillated cellulose (MFC) was introduced. Cellulose nanowhiskers (CNW), however, were prepared from wood through acid hydrolysis as early as 1951 (Ranby 1951).

According to classical mechanics of materials theory (Weibull 1951) the influence of flaws should be reduced by breaking down plant fibres into nanofibrils, since statistically fewer flaws ought to occur in thinner fibres. The theoretical Young's modulus of crystalline cellulose ranges from approx. 124 to 172 GPa (Tashiro and Kobayashi 1985; Eichhorn and Davies 2006; Tanaka and Iwata 2006), depending upon the model used. Recently, using quantum mechanics, the modulus of cellulose I beta has been calculated to be 99.7 GPa (Santiago et al. 2011). Cellulose is a polysaccharide made up of repeating anhydroglucose units which are linked

through the β 1-4 glycosidic bond (an oxygen atom covalently bonded to C1 of one glucose ring and C4 of the adjacent glucose ring) (Klemm et al. 1998) and in plants is found embedded in a matrix of hemicelluloses and lignin (Fig. 1). It has reactive surface hydroxyl groups which are able to form hydrogen bonds.

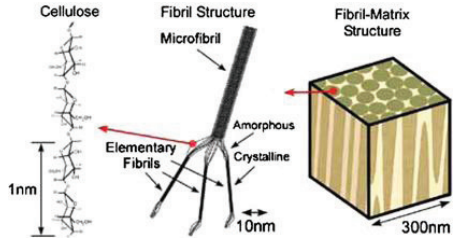

Figure 3. Structure of cellulose fibrils extracted from wood. Reprinted with permission from (Postek et al. 2011) © 2011 IOP Publishing Ltd.

Additionally, the presence of surface hydroxyl groups enables various surface chemical modifications to be carried out. Thus the properties of cellulose can be tailored to suit certain applications which, in turn, provide versatility. Cellulose fibrillation methods are top-down approaches, where the ultrastructure of wood is broken down in order to extract nanocellulose fibrils. The nomenclature of nanocellulose is rather complicated and many terms are used in the literature. Broadly, nanocellulose can be categorized with respect to the aspect ratio of nanofibrils. Mechanically disintegrated nanocellulose from wood pulps is termed microfibrillated cellulose (MFC). If chemical pre-treatments are applied prior mechanical refining, the resulting product is referred to as nanofibrillated cellulose (NFC). The chemical treatment could be also indicated in the term as well, for example, TEMPO-oxidized cellulose nanofibrils (TOCN). Cellulose nanocrystals (CNC) or cellulose nanowhiskers (CNC) are rod-like structures that are obtained through acid hydrolysis of the aforementioned or other cellulosic sources. Similar to CNC is microcrystalline cellulose (MCC) although it has a smaller aspect ratio than CNC. All of these comprise several or tens of cellulose molecules in width,

depending on the preparation method and/or treatments used. A good review on cellulosic particles their preparation and characteristics are given by Siro and Plackett (2010). Wood has approximately 30 – 40 % of cellulose of which around half is in crystalline form (depending on raw material) (Postek et al. 2011).

2.2 Nanocellulose reinforced composites

During the last two decades micro and nanocellulose reinforced composites have been the subject of intensive research and a number of review papers have appeared covering this work (Abdul Khalil et al. 2012; Duran et al. 2012; Moon et al. 2011; Eichhorn et al. 2010; Siro and Plackett 2010; Azizi Samir et al. 2005). Cellulose is very often chemically modified in order to improve the disintegration process, impart special properties, control its hydrophilic nature or for other reasons. The cellulose surface can be functionalised in various ways, such as by acetylation, TEMPO-oxidation, silylation, polymer grafting or polyelectrolyte surface adsorption which facilitates control of the hydrophilic nature of the cellulose molecule as well as imparting new properties. Thus the potential applications of nanocellulose reinforced composites can span a broad range. Functionalised cellulose can be used in many forms (suspension, powder, film, aerogel) and is employed in many different ways (food additive, thickener, binder). Herein, the focus is on nanocellulose which is used in composite materials, thus a short overview of cellulose nanocomposites, which exemplifies the versatility of these novel materials, is given.

There are several different trends in the composition of nanocellulose reinforced composites. Probably the most popular preparation method is a simple mixture of polymer (either synthetic or bio-based) with nanocellulose. Nevertheless, all-cellulose nanocomposites, where amorphous cellulose (dissolved) is reinforced with cellulose crystallites, are of interest as well. Recently, a novel “nanowelding”

method based on the partial surface dissolution of cellulose fibrils was introduced as a way of preparing all-cellulose composites (Yousefi et al. 2011). Additionally, hybrid composites can be prepared using a combination of synthetic reinforcing agent (e.g. carbon nanotubes) and nanocellulose, yielding a conductive material (Yoon et al. 2006; Fugetsu et al. 2008). Tough and strong nanocellulose/montmorillonite composites have been developed through mimicking the structure of nacre (Liu et al. 2011). Moreover nanocellulose has been successfully used in the preparation of flexible magnetic aerogels (Olsson et al. 2010) as well as a nano-sized scaffold (Korhonen et al. 2011). Improvements in fibre-matrix interactions and toughness has been reported for bamboo/PLA/MFC (Okubo et al. 2005; Okubo et al. 2009) and plain woven carbon fibre (CF)/epoxy/MFC composites (Gabr et al. 2010c). A similar effect was observed upon the addition of nanocellulose to urea formaldehyde adhesives (Veigel et al. 2011). Optically transparent bacterial cellulose (BC) and plant-based (wood) cellulose reinforced composites have been shown to have potential as flexible displays in the electronics industry (Yano et al. 2005; Okahisa et al. 2009). The control of fibril-fibrils interaction in nanocellulose through modifications by, for example, DNA grafting (Mangalam et al. 2009) may open up new possibilities in constructing miniature devices through a bottom-up approach. Nonetheless, all advances lead to the formation of cellulose nanocomposites. Thus it is of paramount importance to understand the underlying deformation mechanisms since any material has to sustain loads if used in everyday life.

2.3 Micromechanical models

The simplest model of the Young's modulus of aligned long-fibre composites treats the material as it would consist of bonded parallel slabs. The relative thickness of the slabs is proportional to the volume fractions of matrix and fibres

and they have the same length. If this system is loaded in direction of the fibre alignment, both slabs would exhibit the same strain in the loading direction. Provided that there is no sliding between the matrix and fibre, the Young's modulus can be calculated according to Eq. 1. (Hull and Clyne 1996).

$$E_c = X_r E_r + (1 - X_r) E_m \tag{1}$$

Where E_c is composite modulus; E_r is reinforcement modulus; E_m is matrix modulus; X_r is fibre volume fraction.

This model is often referred to as a *Rule of Mixtures* or *uniform strain*. The theoretical Young's modulus based on the aforementioned model with respect to the volume fraction of reinforcement is shown in Fig. 4.

If the same system is loaded in a transverse direction to the fibres and normal to the plane of the slab interface, the components exhibit uniform stress thus it is called the *uniform stress* model. Then the Young's modulus could be modelled according to Eq. 2. (Hull and Clyne 1996).

$$E_c = \left[X_r / E_r + (1 - X_r) / E_m \right]^{-1} \tag{2}$$

This modelled is also known as Reuss and schematically shown in Fig.4. These two aforementioned models do not fully explain the elastic behaviour of composites but represent two extremes.

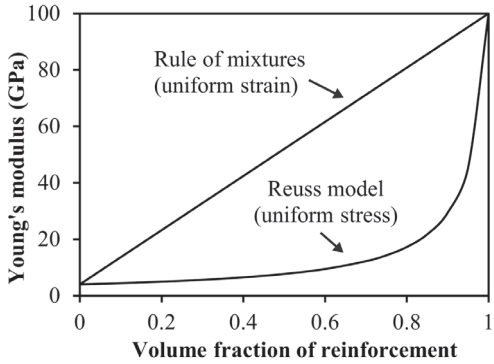

Figure 4. Young's modulus dependency on volume fraction of reinforcement. Rule of mixtures (uniform strain) and Reuss (uniform stress) models.

Theories on the deformation mechanisms in nanocomposites have evolved from the pioneering studies on semicrystalline polymer fibres by Treloar (Treloar 1941), who was the first to discuss the reorientation of polymer materials under extension, as well as Ward (1962) who derived models where crystalline domains were considered in series with amorphous domains. The work of Halpin and Kardos (Affdl and Kardos 1976) gave the basis for predicting the mechanical stiffness of a semicrystalline polymer. It was based on composites theory and strongly influenced by the work of Hill (Hill 1963; Hill 1964), who modelled composites as a single fibre embedded in a cylinder of matrix. Similarly Davies (Davies 1971a; Davies 1971b) modelled the mechanical properties of composites and introduced a modified rule of mixtures, where a correction coefficient was introduced. Takayanagi et al. (1967) proposed a parallel-series model in which the stress in the crystals and in amorphous regions is non-uniform. In this way crystals were overstressed and amorphous zones under-stressed. Thus stress transfer would take in place in these systems at the nano-scale. Percolation theory, developed by Ouali and co-workers (Ouali et al. 1991) is nowadays widely used in the modelling of the mechanical properties of composites. It assumes interactions between fibrils as opposed to the unlike earlier models. Percolation theory dates back to the 1940s

and is related to the assumption that chemical bonds are formed randomly. Basically, it examines whether the elementary segments of a system are macroscopically connected. In a percolated cluster all of the components are in the same state. When the cluster starts dominating in a system it becomes percolated. This point is termed the percolation threshold and it indicates a phase transition. In materials science it usually indicates an abrupt change in the properties of material. From percolation theory, Young's modulus of a composite is expressed as shown in Eq. 3 (Ouali et al. 1991).

$$E_c = \frac{(1-2\psi+X_r)E_m E_r + (1-X_r)\psi E_r^2}{(1-X_r)E_r + (X_r-\psi)E_m} \tag{3}$$

Where E_c is composite modulus; E_r is reinforcement modulus; E_m is matrix modulus; X_r is fibre volume fraction. Where ψ is a percolation volume fraction and given by Eq. 4:

$$\psi = X_r\left(\frac{X_r - X_c}{1-X_c}\right)^b \tag{4}$$

Where X_c is the percolation threshold. A more detailed description of the models applied in the study along with the formulae is presented in **Paper I**.

2.4 Experimental micromechanics

Tools available for investigating of the micromechanics of nanocellulose reinforced composites are limited due to the small size of the individual fibrils. It is not possible to handle nanocellulose fibrils mechanically, thus typical methods, such as fibre pull-out, microbond or single fibre fragmentation (Hull and Clyne

1996), used to study the stress transfer in fibre reinforced composites are not applicable. Techniques such as atomic force microscopy (AFM), X-ray diffraction (XRD) and Raman spectroscopy have been employed to study the strength of single nanofibrils (Cheng et al. 2009; Iwamoto et al. 2009), structure (Oksman et al. 2006) and the stress transfer within nanocomposites (Cooper and Young 1999) respectively. In this study Raman spectroscopy was used to investigate the stress transfer mechanisms in nanocellulose reinforced composites.

2.5 Raman spectroscopy and deformation mechanics

Raman spectroscopy is based on a physical phenomenon - Raman scattering. The greatest advantage of Raman spectroscopy is the ability to examine samples with minimal preparation. Experimentally, Raman scattering was first observed by Raman and Krishnan in 1928 (Raman and Krishnan 1928). When a molecule is subjected to monochromatic light (laser), electrons and nuclei are forced to shift in opposite directions, thus a dipole moment is induced and a short-lived (virtual) molecular state is created. The dipole moment is proportional to the strength of the electric field and the molecular polarizability (i.e. chemical bond). When the molecule relaxes from its virtual state it emits a photon and returns to a different vibrational state from the initial state. The difference between the initial state and the new state leads to a frequency change of the emitted photon compared to the photon of the incident light. This different frequency can be detected and assigned to a Raman band. The Raman band is specific to chemical bonds and symmetry of a molecule. Hence, every molecule has a pattern of Raman bands which allows identification. Symmetric vibrations give the largest changes in the polarizability and consequently more intensive Raman scattering. Moreover, if a molecule is subjected to mechanical deformation, vibrational frequencies change thus

deformations can be detected. More detailed information can be found in Smith and Geoffrey (2005).

A typical Raman spectrum of MFC is shown in Fig. 5. Intense vibrational bands correspond to CH, HCO (~ 2800 cm^{-1}) and COC (~ 1095 cm^{-1}) vibrations (Gierlinger et al. 2006; Wiley and Atalla 1987).

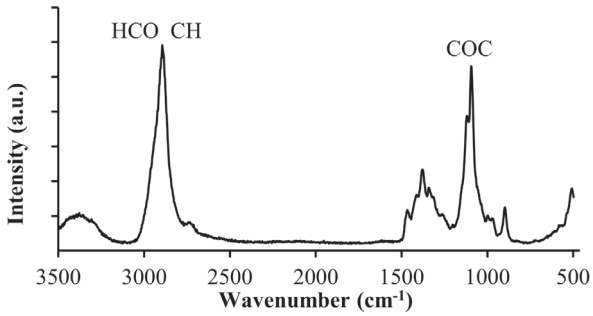

Figure 5. Raman spectrum of MFC.

One of the first studies on unstrained natural fibres was by Blackwell et al. (1970), who reported Raman spectra from algae. The Raman spectra from the natural materials such as wool, silk, hair and feather has also been reported (Hogg et al. 1994; Edwards et al. 1997; Akhtar et al. 1997) as well as band assignments of celluloses (Wiley and Atalla 1987).

Raman spectroscopy has been shown to be a useful, non-invasive, tool for studying the in-situ micromechanics of polymers (Young et al. 1990; Davies et al. 2001), particulate composites (Cooper and Young 1999; Shyng et al. 2006), carbon nanotube reinforced composites (Cooper and Young 1999; Cooper et al. 2001) and cellulosic materials such as wood fibers (Gierlinger et al. 2006; Eichhorn et al. 2001; Eichhorn et al. 2000; Peetla et al. 2006), cotton (Quesada Cabrera et al. 2011) and cellulosic nanocomposites (Rusli et al. 2010; Rusli et al. 2011; Pullawan et al. 2010; Eichhorn and Young 2004). The use of Raman spectroscopy to study deformation in polymer single crystals was pioneered by Mitra and co-workers

(Mitra et al. 1977). They concluded that frequency shifts in the spectra obtained from single crystals of diacetylene take place due to bond anharmonicity. A later study by Batchelder and Bloor (1979) supported the findings of Mitra and colleagues. When the molecular chain is strained by external load the atoms are displaced from their original positions by an amount proportional to the force. As the cellulose crystallite is stretched along the axis, the skeletal chain is mainly deformed by the mechanism of ring deformation in conjunction with stretching and bending of β-1,4-glycosidic linkage as well as stress distribution via hydrogen bonding (Tashiro and Kobayashi 1985; Hinterstoisser et al. 2003). As a result a Raman band initially located at ~1095 cm^{-1}, assigned to C-O-C stretching (Gierlinger et al. 2006; Wiley and Atalla 1987), shifts towards a lower wavenumber position, due to direct deformation of the cellulose backbone (Eichhorn et al. 2001; Eichhorn et al. 2000; Eichhorn and Young 2001; Eichhorn et al. 2001; Eichhorn et al. 2001; Bakri and Eichhorn 2010). The shift rate directly corresponds to the stress transfer in a composite. Thus it allows in-situ studies of molecular deformations and provides valuable insight towards the micromechanics of composites.

2.6 Structure and thermomechanical properties of composites

The structure of a polymer changes significantly when nanocellulose is added. Firstly, it introduces heterogeneity, secondly, it changes the crystallization behaviour of a polymer. Studying the thermomechanical properties is a good way to evaluate the structure of nanocomposites and is very important as composites undergo temperature cycles during their service life. In dynamic mechanical thermal analysis (DMTA) samples are subjected to an oscillating sinusoidal load at a particular frequency upon heating. The applied stress varies as a function of time and so does the strain. In viscoelastic materials, strain lags behind the stress. Thus

the variation in stress and strain with respect to time can be expressed as shown in Eq. 5 and Eq. 6 respectively (Young and Lovell 1991).

$$\sigma = \sigma_0 \sin(\omega t + \delta) \tag{5}$$

$$e = e_0 \sin \omega t \tag{6}$$

Where σ is applied stress; σ_0 is amplitude of the stress; t is time; ω is angular frequency (2π times the frequency in Hz); δ is a phase angle (phase lag); e is strain; e_0 is amplitude of the strain.

As a result two dynamic moduli can be defined: storage modulus E' (Eq. 7) and loss modulus E" (Eq. 8) (Young and Lovell 1991).

$$E' = (\sigma_0 / e_0)\cos\delta \tag{7}$$

$$E'' = (\sigma_0 / e_0)\sin\delta \tag{8}$$

They represent elastic and plastic (damping) properties respectively. The ratio E" over E' is termed Tan δ. One of the advantages of the DMTA technique is the possibility to relate peaks in the E" and Tan δ curves to certain molecular motions (Young and Lovell 1991; Brown 2001). Dynamic scanning calorimetry (DSC) can be used in a similar way to follow molecular transitions upon heating and cooling. This technique provides insights into the crystallization behaviour of a polymer. There have been a number of studies on the behaviour of PLA upon the addition of nanocellulose (Oksman et al. 2006; Nakagaito et al. 2009; Suryanegara 2010, Suryanegara et al. 2009; Tingaut et al. 2010; Pei et al. 2010; Lin et al. 2011, Jonoobi et al. 2010a, Kvien et al. 2005; Mathew et al. 2005) just to name a few. The potential of cellulosic fillers to act as a nucleating agent and enhance thermal

stability and stiffness of a polymer have been reported previously (Suryanegara 2010; Pei et al. 2010; Mathew et al. 2005). Nevertheless, the growth of crystals is affected by a number of factors, such as surface energy and surface roughness (Quan et al. 2005), thus further investigations are needed.

3 EXPERIMENTAL

The main materials, such as the cellulose fibrils and polymers, used in the preparation of the composite films are described in section 3.1. Methods employed in the study are presented in section 3.2. More detailed information can be found in **Papers I-V**.

3.1 Materials

3.1.1 Cellulose fibrils

The cellulosic materials used in this study were prepared at the department of Forest Products Technology, Aalto University, Finland. Microfibrillated cellulose was disintegrated from never dried bleached birch Kraft pulp in an ultra-fine friction grinder (Masuko Supermasscolloider, model MKZA 10-15J) without any chemical modification. The pulp suspension was passed five times (**Paper I**) and seven times (**Paper II**) through the grinder. The suspension was in the form of a gel and had solids content of approximately 2 wt%.

TEMPO-oxidized fibrillated cellulose (TOFC) (**Paper III, IV, V**) was prepared from never dried bleached birch Kraft pulp according to the method detailed by Saito and co-workers (Saito et al. 2006). After the oxidation, the fibrils were stirred in a commercial blender with the addition of deionized water until a transparent gel, which had a solids content of approximately 0.5 wt%, was formed. No additional filtration, or any other treatment, was carried out. The term nanocellulose is used hereafter to refer to both MFC and TOFC although they both consist of nano and micro fibrils.

3.1.2 Polymeric matrices

Two types of water soluble poly(vinyl) alcohol (Elvanol 71-30 and Elvanol 75-15), manufactured by DuPont, Wilmington, Delaware, USA, were used as matrix (**Paper I**). Elvanol 71-30 is a fully hydrolyzed polymer with an average molecular weight (M_w) of ≈ 93700. Elvanol 75-15 is a hydrolyzed copolymer of poly(vinyl) alcohol and methyl methacrylate (MMA) with an average M_w of ≈ 65500.

Poly(lactic) acid (NatureWorks 2002D) manufactured by NatureWorks, Minnetonka, MN, USA was used as a matrix in **Papers II-V**. The matrix had to be transparent to visible light in order to use Raman spectroscopy in studying the stress transfer mechanisms in nanocomposites.

3.2 Methods

3.2.1 Cellulose chemical modification

Acetylation of MFC. MFC was solvent exchanged to ethanol and then to toluene by two subsequent centrifugations at 8000 rpm for 15 min at 20 °C. The suspension was decanted and fresh media added after each centrifugation. Acetic anhydride (AA) was added to the resultant MFC suspension in toluene and maintained at a temperature of 105 ± 5 °C for 15 and 30 minutes. Approximately 100g of AA was added to react with 1.5 g of cellulose (dry weight). The reaction was quenched by placing the flask into an ice bath and adding acetone to the mixture. Suspensions of acetylated MFC were centrifuged as previously described and then solvent exchanged to chloroform. The final acetylated MFC suspension had a solid content of ~ 1 wt% and was used in the preparation of the composite films (**Paper II**).

Acetylation of TOFC. The acetylation of TOFC was similar to that of MFC but the TOFC was exchanged to dimethyl formamide (DMF) where the acetylation reaction took place (**Paper III-IV**). The reaction was carried out for 15 and 120

minutes (**Paper III**) at 105 ± 5 °C. In **Papers IV-V** the suspension of TOFC in DMF was pre-heated to 125 ± 5 °C prior to the addition of AA in order to boil away any remaining water. Then the acetylation reaction took place at 125 ± 5 °C for 45 min. It was stopped by placing the reaction flask in an ice bath and adding acetone. The whole mixture was centrifuged and the media decanted off. Final suspensions in chloroform (~ 0.3 wt%) were used in the preparation of the composites.

3.2.2 FT-IR spectroscopy

Infrared spectroscopy is based on the absorbance of energy at the resonant frequency of molecules. When photons of incident light (infrared) hit the sample the energy is absorbed due to molecular vibrations which are bond and vibrational mode dependent. Thus it is possible to detect the presence of certain bonds in turn organic compounds. The IR technique is water sensitive unlike Raman spectroscopy, since it is related to changes in dipole moment. Vibrational bands from the carbonyl (C=O) groups appear at ~ 1740 cm^{-1}, and indicate the presence of acetyl moieties. Thus this technique is suitable for detecting ester groups on cellulose surfaces. Acetylated and non-acetylated samples were dried in an oven and spectra collected between 400 cm^{-1} and 4000 cm^{-1}. The spectrometer was equipped with a laser operating at a wavelength of 632.8 nm. A photoacoustic cell was used in the study (**Paper II-IV**).

3.2.3 Atomic force microscopy (AFM)

The technique is based on the interaction forces between atoms. The tip, which is attached to a cantilever, is either brought into contact with the surface or is oscillated over it. Due to the tip-surface interactions, topography features are

recorded. During the preparation of samples a dilute suspension of nanofibrils is spin coated on a substrate. They are adsorbed on the surface thus the identification and measurement of individual nanofibrils is possible. Tapping mode was used in the studies i.e. the tip oscillates at its resonance (or near resonance) frequency and comes into contact with the specimen surface intermittently. Mechanical contact of the tip with sample surface is minimized, eliminating inelastic deformation of the specimen, thus, rendering the technique suitable for the analysis of soft materials. Films were imaged with a Nanoscope IIIa multimode scanning probe AFM. (**Paper II, IV**).

3.2.4 Preparation of composite films

Preparation of the composites essentially varied with respect to the matrix used. Water soluble PVA was used in **Paper I** therefore cellulose suspended in water was directly mixed with the polymer. Later studies (**Paper II-V**) dealt with a water insoluble polymer – PLA, thus the cellulose had to be chemically modified and solvent exchanged as described in section 3.2.1.

PVA was dissolved in hot water at +80 ±5 °C under constant agitation for 60 min. The solution was left to cool down and the MFC added, to prepare composites to weight fractions of 1, 5, 10 and 15 %. The suspension was mixed for 2 h. Three different concentrations were used: 1, 2 and 4 %. Composites were named A, B, C accordingly. Then the suspensions were cast without degassing (composites A1, B1, C1) or with (composite B3) in order to study the influence of vacuum. For example, composite B3 was prepared by mixing 2 wt% concentration polymer solution with a certain amount of MFC (0, 1, 5, 10, 15 wt%) and then the cast was degassed for 20h. The PVA polymer, Elvanol 75-15, was used to study any effect of mixing time on composite quality, thus two different mixing durations were chosen, 2 and 24 h (**Paper I**).

In **Papers II-V** cellulose was acetylated prior to mixing with the PLA solution in chloroform. Either acetylated MFC (**Paper II**) or acetylated TOFC (**Paper III-V**) was added to the PLA solution, homogenised and degassed prior casting onto a release agent treated glass plate. The casts were left in a well-ventilated environment overnight and then finally cured in an oven at 60 °C for 30 minutes. Pure PLA films were also prepared as well as pure cellulose film (**Paper IV**).

3.2.5 Mechanical testing

Mechanical testing was performed according to the standard *ISO 527-1996* (Plastics. Determination of tensile properties). Specimens were punched out of the films using a custom made cutting die (type 1 BA). The specimens were conditioned in accordance with *EN ISO 291:2008* (Plastics. Standard atmospheres for conditioning and testing) at +23 °C ±1 °C and 50% ±2% relative humidity (RH) prior testing. To study effect of RH on the mechanical properties of the composites (**Paper I**), the following RH were used: 45 % ±1, 50 % ±1 and 55 % ±1. The samples were kept for at least 72h in the controlled environment prior each test. The tests were carried out on MTS 400/M testing rig at the same temperature and RH as the conditioning setting prior to the test. Testing speed was 20 mm/min for composites with the PVA matrix and 5 mm/min for composites with the PLA matrix. A load cell of 50 N was used in all cases. The tensile speed in the Raman measurements was 0.05 mm/min and a load cell of 2 kN was used.

3.2.6 Dynamic mechanical thermal analysis (DMTA) and differential scanning calorimetry (DSC)

Composite films were cut into strips having a nominal width of 5.3 mm and a length of ~ 12 mm. The samples were tested in tension in a Q 800 (TA Instruments) dynamic mechanical thermal analyser. The temperature varied

between 0 and + 250 ºC at a heating rate of 3 ºC/min. Data were recorded at equilibrium for 2 seconds at each step. The Oscillating frequency was 1 Hz.

Dynamic mechanical analysis (DMA) with humidity control was carried out on the same device as described above, but equipped with a humidity control chamber. The relative humidity (RH) was cycled between 0 and 90 % under isothermal (30 °C) conditions. The stabilization time was 240 min at both RH levels.

DSC is used in to monitor molecular transitions in polymer and to indirectly evaluate crystallinity. The temperature of a sample is increased as a function of time. Samples having a weight of 6 – 10 mg were sealed in crucibles and heated from 25 to 200 °C at a rate of 20 °C/min. This was followed by a cooling stage where the temperature was decreased at a rate of 10 °C/min until it reached 0 °C. Finally, a second heating stage at a rate of 10 °C/min was carried out. More details can be found in **Paper V**.

3.2.7 Scanning electron microscopy (SEM)

Scanning electron microscopy was employed to study the topography of the fracture surfaces of the composite films. Imaging is based on the detection of secondary electrons, thus limiting it exclusively to surface features. The fracture surfaces of the samples were imaged after mechanical testing. Three electron microscopes were used: a table-top SEM (Hitachi TM-1000) (**Paper I**); a Zeiss supra 40 (**Paper II, IV**) and a Leo (Zeiss) 1450 (**Paper III**). All of the samples were gold sputtered prior to imaging.

3.2.8 Raman spectroscopy and imaging

Raman spectroscopy was used for two purposes: i) to study composition of the specimens and ii) to detect stress transfer from the matrix to NC fibrils. Stress-free composite films were embedded in epoxy and left to cure for 24 h. Then a smooth

cross-sectioned surface was created using a Leica ultramicrotome (Leica Microsystems, Wetzlar, Germany). The sample was placed under a microscope equipped with a Raman detector and a laser operating at a wavelength of 532.24 nm. The basic principle behind the Raman imaging is shown in Fig. 6. The area of interest is scanned pixel-by-pixel at a spatial resolution of 1-2 µm and a spectrum is recorded in each pixel. Construction of the Raman images is based on a difference in band intensities arising from a variance in the quantity of material constrained in the sample, i.e. relation proportional to cellulose and PLA.

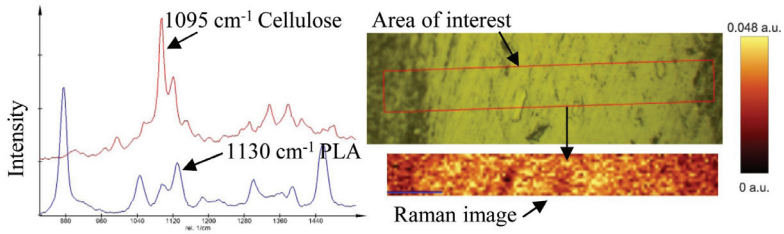

Figure 6. Basic principle of Raman imaging.

A band located at ~ 1095 cm^{-1} is characteristic of cellulose and a band located at 1130 cm^{-1} is characteristic of PLA. By taking the intensity ratio (background corrected) of the two a "chemical map" is formed (Fig 6). Previously Raman imaging has been employed to study the chemical composition of the wood cell wall (Gierlinger and Schwanninger 2007) as well as the molecular orientation in native cellulose fibres (Atalla et al. 1980).

In order to detect stress transfer in the composites, the films were placed under load. Samples were deformed stepwise in a tensile rig and Raman spectra were recorded at each point. The strain increment between two steps was 0.1 %. The shift in the Raman band located at ~ 1095 cm^{-1} was of interest since this can be related to the molecular deformation of the cellulose molecule. The shift was calculated after mixed Gaussian/Lorentzian peak fitting. Further details can be found in **Paper IV** and in a review paper by Young and Eichhorn (2007).

3.2.9 Additional techniques

Details of the determination of the degree of substitution (DS) can be found in **Papers II-IV.** Composite density measurements were performed by cutting circular disks (either 5 or 10 mm in diameter) from the films, weighing them and measuring the thickness (**Paper I**). A pH meter (Metrohm 744 pH) was used to measure the pH of PVA (**Paper I**). The viscosity of PVA water solutions at room temperature was measured using a capillary viscometer (**Paper I**).

4 RESULTS AND DISCUSSION

4.1 Morphology of nanocellulose and degree of substitution

It is hard to define the morphology of nanocellulose precisely as it is a mixture of nano and micro fibrils (if not filtered) which are also entangled. A SEM image of an MFC suspension in water upon drying (Fig. 7) illustrates the entangled structure, although slightly aggregated due to drying under vacuum.

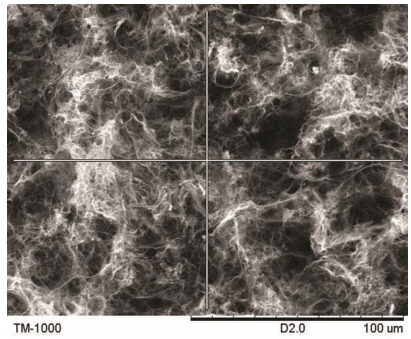

*Figure 7. SEM micrograph of MFC (**Paper I**).*

Micro-sized fibrils are approximately of 200 microns in length and around 4 microns in width (aspect ratio ~ 50) as measured from polarized light micrographs of diluted MFC suspensions in water (**Paper I**). The aspect ratio of nanofibrils spans a wider range from ~ 20 to 150 as measured from the height profiles of an AFM topography image (Fig. 8).

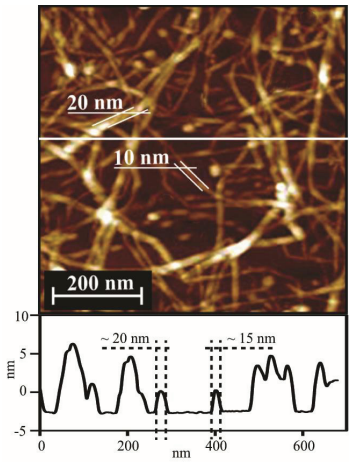

*Figure 8. AFM topography image of spin coated MFC. The height profile of the marked area (white line) is shown below the topography image (**Paper II**).*

The widths are approximately 10 – 20 nm as the topography image and height profile indicate (Fig. 8). Micro-sized fibrils in the MFC suspension scatter light, thus the suspension is not transparent to visible light. The transparency of the TOFC water suspension indicates better dispersion and the smaller size of the fibrils (Fig. 9).

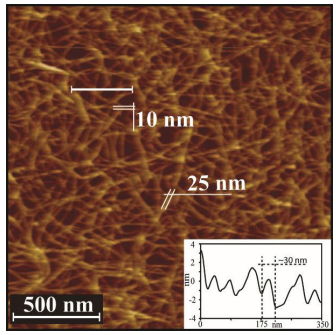

*Figure 9. AFM topography image of spin coated TOFC. The inset shows the height profile of the marked area (white line) (**Paper IV**).*

The widths of TEMPO-oxidized fibrils are approximately 10 – 25 nm and the length is in the range of ~ 1 µm. However, aggregation of the TOFC fibrils takes place when the media is changed from a polar to a non-polar, even after chemical modification. This has the effect of slightly decreasing the aspect ratio of the TOFC

fibrils (**Paper IV**). A term nanocellulose (NC) is used, thereafter, for both MFC and TOFC.

Acetylation of MFC was found to be reaction time dependant. The DS was found to be 0.24 and 0.43 after 15 min and 30 min reaction time respectively (**Paper II**). In the case of acetylated TOFC the DS was 0.6 after 15 min and 0.4 after 120 min reaction time (**Paper III**), although it reached 0.98 after 30 min reaction time (**unpublished data**). A modified acetylation method was used in **Paper IV**, however it yielded a DS of 0.16 after 45 min acetylation of TOFC and a DS of 0.11 when birch pulp was acetylated. The DS of MFC and TOFC cannot be compared directly as the media and chemical modification method differed slightly.

4.2 Influence of the preparation method on the mechanical properties of composites

Cellulose is well known for its hydrophilicity, thus it acts as a thickener in water-based suspensions. When NC is mixed with a polymer dissolved in water the NC increases the viscosity of the mixture and consequently the dispersability of the NC. The dispersion of low weight fractions of nanocellulose is better at slightly higher polymer concentrations, however, when a threshold of around 10 wt% load of nanocellulose is attained, lower polymer concentration solution favours dispersion. The mechanical properties of the composites are affected accordingly (Fig. 10).

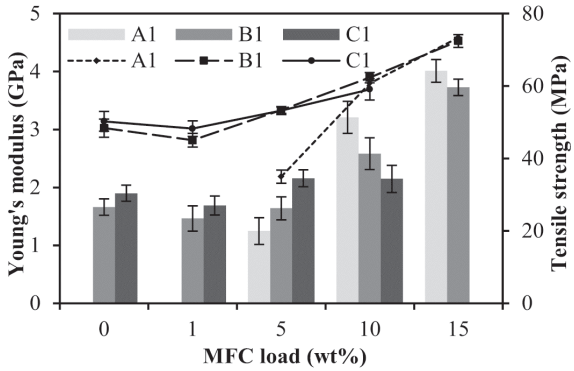

*Figure 10. Influence of solution concentration and MFC loading on mechanical properties of MFC reinforced PVA composites. Columns represent Young's modulus; curves tensile strength. Standard deviation is depicted by error bars. A1, B1 and C1 – 1, 2 and 4 wt% PVA solution concentrations respectively (**Paper I**).*

In fact, preparation of 1 wt% polymer concentration composites with 1 wt% MFC load was not possible, since MFC formed lumps at the end of the curing process. The Young's modulus of C1 composites (PVA solution concentration 4%, degassed) was the highest at 5 wt% load, although it significantly decreased at 10 wt% load and exhibited the lowest Young's modulus value compared to the others. Composite A1 (PVA solution concentration 1%, degassed) had the lowest tensile strength at 5 wt% load of MFC, but was equal to that of B1 (PVA solution concentration 2%, degassed) and C1 at 10 and 15 wt% loads. The preparation of C1 composite with 15 wt% load was not possible due to the high viscosity. Clearly the viscosity affects dispersion and consequently mechanical properties, since the good distribution of reinforcing agent is very important as has been stated by many workers (Favier et al. 1995; Garcia et al. 2006; Zimmermann et al 2004; Chakraborty et al. 2006; Lu et al. 2008; Cheng et al. 2007; Favier et al. 1997).

Degassing is often used in the preparation of composite films in order to remove entrapped air. As Fig. 11 shows this also affects the Young's modulus of composite films.

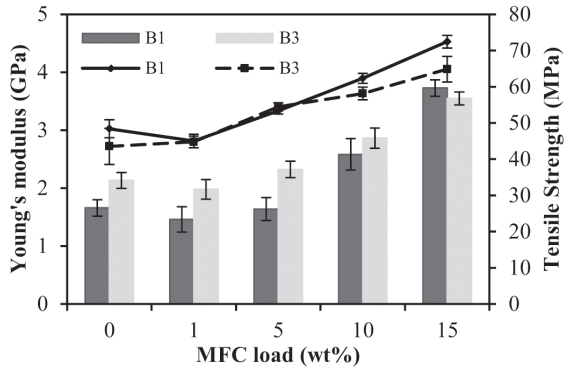

*Figure 11. The effect of degassing on PVA/MFC composite mechanical properties. Concentration of PVA solution in water – 2 wt%. Composite B1 – non degassed; B3 – degassed (**Paper I**).*

At a PVA concentration of 2wt% it was found that the application of a vacuum increases Young's modulus, but MFC weight fraction's above 10 wt% result in a reduction. The amount of air, which can be effectively removed from the polymer-MFC dispersion, is related to viscosity which is linked to the MFC load. The opposite trend was observed when the PVA solution concentration was 4 wt% (**Paper I**). The density of composites has not changed after degassing (**Paper I**), thus the differences in the Young's modulus and tensile strength with respect to degassing are not affected by the density. Another important factor to consider in the preparation process is the mixing time of polymer/nanocellulose blend. An agitation time of 24 h negatively affects both the Young's modulus and tensile strength of composites compared to agitation for 2 h. Long mixing time has been found to be detrimental in both pure PVA films as well as in MFC/PVA composites with 1 and 2 wt% loads (**Paper I**). All-in-all the stiffness and tensile strength of the MFC/PVA composites were improved upon the addition of 5, 10 and 15 wt% loads of MFC. This implies that the percolation threshold is around 5 wt% for this type of composite.

4.3 Dependency of composites morphology on DS of nanocellulose

The dispersion of polar cellulose within a non-polar PLA matrix is virtually impossible (Ljungberg et al. 2005; Heux et al. 2000). The aim of chemical modification was to increase the hydrophobicity of nanocellulose which would result in better dispersion of the cellulose fibrils within the matrix and thus improve the mechanical properties of the composites. The study has shown that visible cellulose aggregates form at lower values of DS (Fig. 12).

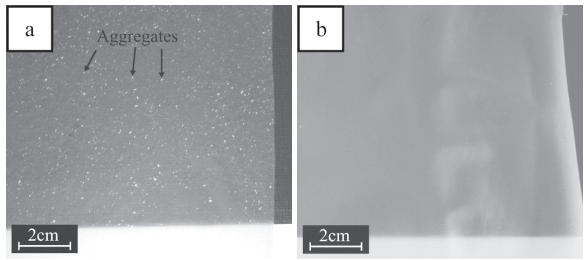

*Figure 12. Photographs of PLA/MFC composites with 20 wt% MFC load (a) DS 0.24 and (b) DS 0.43 (**Paper II**).*

In a PLA/MFC composite film, containing 20 wt% of MFC, a DS of 0.24 was not enough to prevent cellulose aggregation completely (Fig. 12a). However, at as DS of 0.43 the dispersion was much better as no visible MFC aggregates were detected (Fig. 12b). Further, the dispersion of MFC having a DS of 0.43 was studied at higher resolution using Raman spectroscopy. The intensity of a characteristic Raman band correlates with the quantity of material within composite (Quero et al. 2010) (**Paper II, IV**). Thus it could be used to study cellulose dispersion within a PLA matrix. The Raman band characteristic to cellulose, situated at ~ 1095 cm^{-1}, was chosen for comparison with the characteristic band of PLA situated at ~ 1130 cm^{-1}. The Raman images (Figs. 13 and 14) represent a “chemical map”. Each pixel in the image shows the ratio between the aforementioned intensity bands, thus clearly corresponding to quantity of the material.

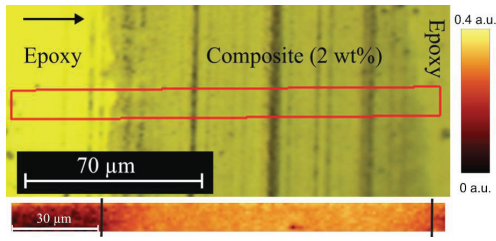

*Figure 13. Microscope image of a 2 wt% MFC (DS 0.43) composite film embedded in an epoxy matrix and a Raman image (below) representing the area within the rectangle. The scale bar in arbitrary units is on the right hand side. Vertical black lines denote the boundaries of the composite film. The arrow indicates the polarization direction of the laser (**Paper II**).*

The lighter colour in Figs. 13 and 14 correspond to higher amounts of cellulose, thus the Raman image appears lighter in Fig. 14. Some aggregates, which are marked with arrows (Fig. 14), can be seen at 20 wt% load of TOFC. Good dispersion of reinforcement agent is limited at higher weight fractions due to fibril-fibril interaction i.e. the fibrils start to aggregate due to the formation of hydrogen bonding between adjacent cellulosic surfaces. Extensive fibril-fibril interactions take place when the load of a reinforcement agent exceeds the percolation threshold. Consequently there are discrepancies between modelled (which usually assume perfect dispersion) and actual values of Young's modulus as shown in **Paper I**.

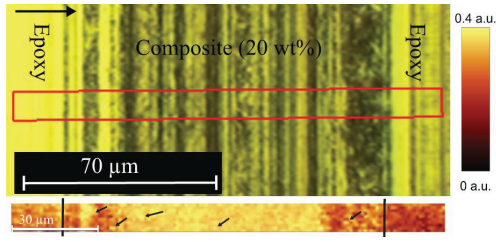

*Figure 14. Microscope image of a 20 wt% MFC (DS 0.43) composite film embedded in epoxy matrix and a Raman image (below) representing the area within the rectangular. The scale bar in arbitrary units is on the right hand side. Vertical black lines denote boundaries of the composite film. The arrow indicates polarization direction of the laser (**Paper II**).*

Raman imaging showed clustering of cellulose fibrils which were not visible to the naked eye, thus providing a high resolution (~ 1-2 µm) tool to study nanocellulose dispersion within polymer matrices. Although the resolution is not higher than that of visible light microscopy, the ability to distinguish materials and evaluate their quantity at micro-scale provides advantages.

4.4 Mechanical behaviour of the nanocomposite films

The mechanical behaviour of composite films was altered upon the addition of both MFC and TOFC to the polymer matrices (**Paper I-V**). Typically (Zimmermann et al. 2004; Chakraborty et al. 2006; Lu et al. 2008; Cheng et al. 2007; Roohani et al. 2008, Cheng et al. 2009) an improvement in Young's modulus and tensile strength are accompanied by a decrease in strain-to-failure. This behaviour was observed upon the addition of MFC to a PVA matrix (**Paper I**). The behaviour of a brittle polymer matrix – PLA was modified in a different manner to PVA. Toughening was observed at low weight fractions of reinforcing agent, but reinforcement occurred at higher weight fractions (Fig. 15).

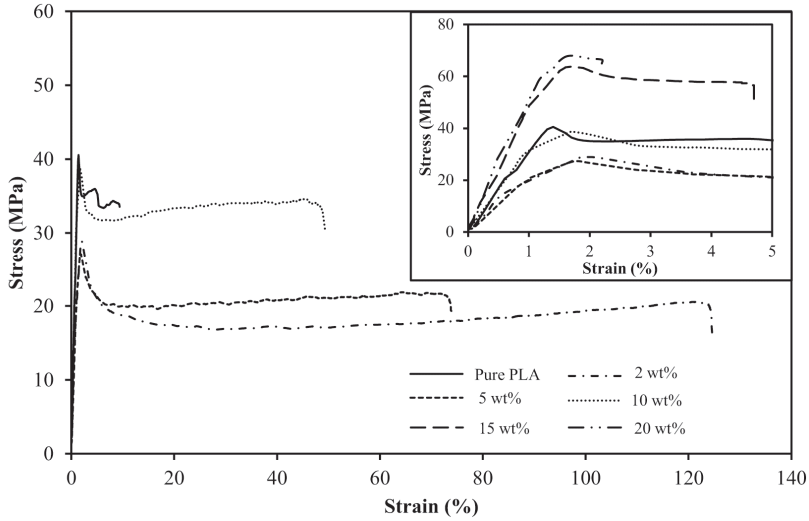

*Figure 15. Representative stress – strain curves of pure PLA and PLA/MFC composites (DS 0.43). The stress – strain curves in a region below 5% of strain are shown in the inset (**Paper II**).*

The DS of nanocellulose affected the deformation mechanisms in both MFC (**Paper II**) and TOFC (**Paper III**) reinforced composites. Higher DS led to greater toughening. The toughness, expressed as tensile energy absorbed (TEA) and which is calculated as the area under a stress-strain curve up to the failure point, of PLA/MFC composites was improved by ~ 600 % at 2 wt% load of MFC having a DS of 0.43. The incorporation of 10 wt% of this MFC resulted in improved Young's modulus (by 15 %) and toughness (5 times). An increase in strain-to-failure for composites reinforced with MFC having a DS of 0.24 was observed only at 2 wt% load (**Paper II**) and in the case of TOFC only at 1 wt% load of MFC at both DS (**Paper III**). The improvement in toughness can be attributed to an increase in the crazing (Fig. 16) owing to the incorporation of MFC (**Paper II, III**).

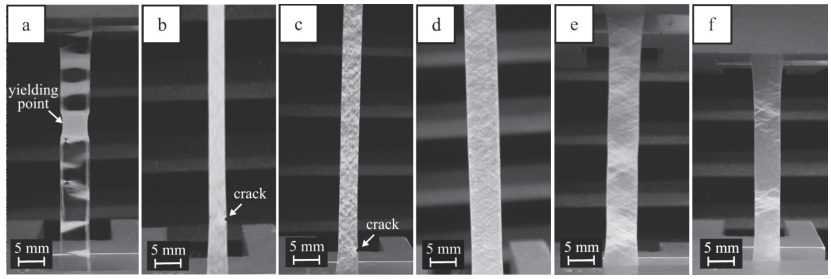

*Figure 16. Crazing in pure PLA film (a) and acetylated MFC (DS 0.43) reinforced composites with weight fractions of: (b) 2 %, (c) 5%, (d) 10 %, (e) 15 %, (f) 20 %. Images were taken right before the fracture, thus the strains were close to the ultimate strain-to-failure values i.e. approx. (a) 9.5 % (b) 120 %, (c) 70 %, (d) 45 %, (e) 4 %, (f) 2 % (**Paper II**).*

The crazing - stress whitening - was observed in both MFC and TOFC reinforced PLA composites. Nanocellulose introduces heterogeneity into a polymer matrix and, due to significant differences in the Young's modulus of the cellulose and the matrix, shear-yielding could be induced, resulting in crazing. Additionally, the introduction of voids into composite films could facilitate inter-fibril debonding and nanofibril slippage as has been reported in pure nanocellulose structures

(Henriksson et al. 2008). This could account for the improved toughness compared to pure PLA. The lower number of hydrogen bonds following esterification would facilitate debonding and slippage and explain the dependency of deformation mechanisms on DS, in addition to dispersion. SEM micrographs of PLA/MFC and PLA/TOFC composite illustrate that plastic deformation takes place in a composite film during mechanical loading (Fig. 17).

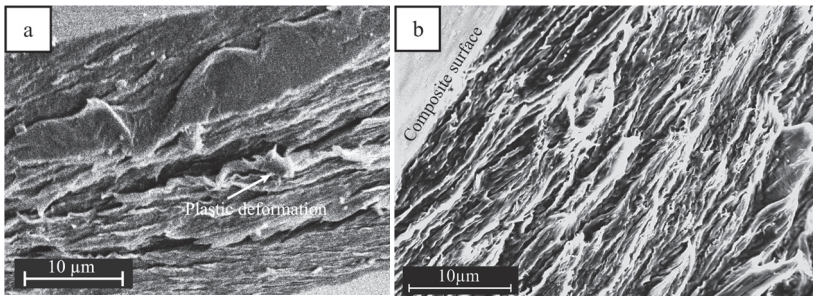

*Figure 17. SEM micrographs of composite fracture surfaces: (a) PLA/TOFC composite with 1 wt% load of TOFC (DS 0.6) (**Paper III**), (b) PLA/MFC composite with 2 wt% load of MFC (DS 0.43) (**Paper II**).*

The toughening effect of nanocellulose on brittle polymers has been reported previously (Okubo et al. 2009; Gabr et al. 2010a; Gabr et al. 2010b; Gabr et al. 2010c) although some other studies (Pei et al. 2010; Jonoobi et al. 2010b; Tome et al. 2011) have reported the opposite i.e. the addition of nanocellulose has rendered polymers more brittle. The present study shows that it is clearly related to the morphology of nanocellulose, since different weight fractions of MFC (**Paper II**) compared to TOFC (**Paper III**) were needed to observe the toughening, as well as DS and dispersion of the reinforcing agent within the matrix.

4.5 Raman spectroscopy and micromechanics

The stress transfer in composites having higher weight fractions (15, 20, 25 and 30 wt%) of TOFC as well as the orientation of the nanofibrils were studied using

Raman Spectroscopy. Orientation is very important since polarizers are used to receive the strongest signal from the fibrils which are parallel to the axis of the sample. The orientation of the TOFC within the matrix was found to be random (**Paper IV**) thus Raman spectroscopy could be applied in studying the stress transfer. Typical deformation induced shift of the Raman band located at ~ 1095 cm^{-1} is shown in Fig. 18.

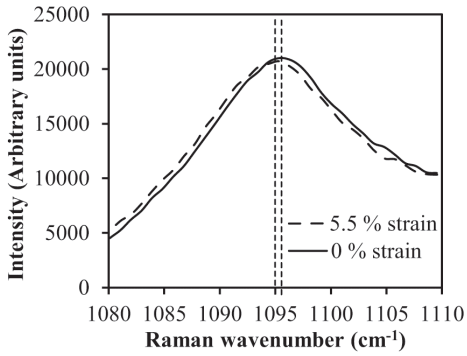

*Figure 18. Typical deformation induced shift of the Raman band from cellulose located at ~ 1095 cm^{-1} for a composite with 30 wt% load of TOFC (**Paper IV**).*

The Raman band shifted towards a lower wavenumber by 0.6 cm^{-1} upon 5.5 % strain in the composite with 30 wt% load of TOFC. The shift itself represents molecular deformations of the cellulose molecule and the gradient of the fitted curve (Fig. 19) shows shifting rate which is directly related to stress transfer within the composite. Fig. 19 shows the Raman band shift with respect to strain at different weight fractions of TOFC.

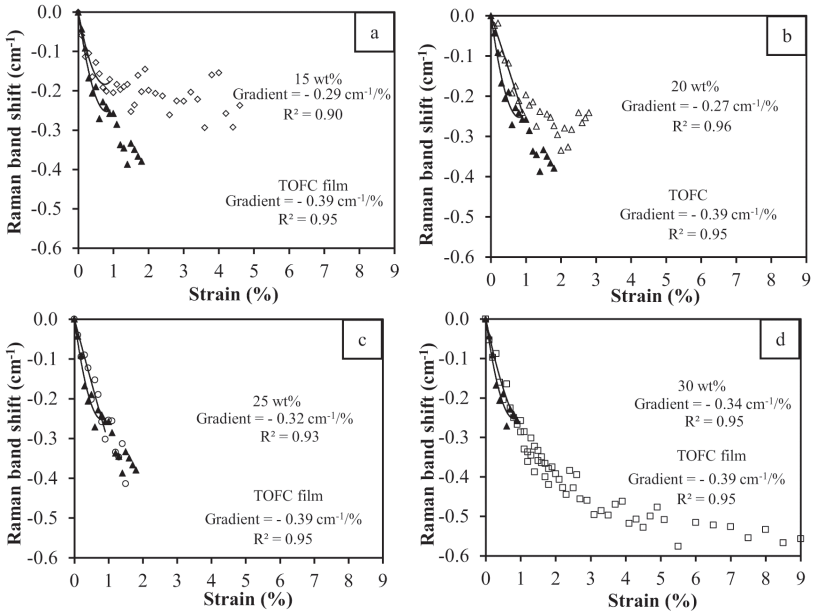

*Figure 19. Shifts in the peak position of the Raman band located at ~1095cm^{-1} for TOFC/PLA composites with different weight fractions of TOFC: a) 15 % b) 20 % c) 25 % d) 30 % as a function of strain (unfilled symbols) compared with data obtained from pure acetylated TOFC films (filled triangles). Data are fitted (up to a strain of 0.9%) using a quadratic equation (solid lines) and the slopes determined from the first derivative of this fit solved at a strain = 0.3 % (**Paper IV**).*

The shift rate increases from 0.29 cm^{-1}/% to 0.34 cm^{-1}/% with respect to the weight fraction (from 15 to 30 %) of TOFC. The strain-to-failure of the composites with 15 and 30 wt% loads of TOFC (even if not all specimens were deformed to fracture) is significantly higher compared to the other composites and the pure cellulose film. This implies different deformation mechanisms. The shifts in composites with 15 and 30 wt% loads plateau at strains over ~ 1% thus indicating debonding between matrix and fibrils which effectively hinders the stress transfer from matrix to nanocellulose fibril. Higher strains to failure could be attributed to frictional sliding. The shift rate, shown as the gradient of the initial linear portion of the stress-strain curve (Fig. 19), in composites with lower weight fractions (15, 20 %) is significantly lower than the shift rate in the pure TOFC film, nevertheless, it gradually converges at 25 and 30 wt% loads, suggesting a network dominated

stress transfer mechanisms (i.e. fibre-fibre interactions and uniform strain). This type of dense network is expected to show "Cox-like" uniform strain behaviour (Cox 1952) within themselves similar to a "composite within a composite" (I'Anson and Sampson 2007). The lower shift rate in composites with 15 and 20 wt% loads of TOFC indicates poor stress transfer to the fibrils. This implies that the percolation threshold was not met at the aforementioned loads of TOFC. It has been reported previously that the Raman band at ~ 1095 cm^{-1} shifts at rate of -2.4 cm^{-1}/% with respect to strain in tunicate cellulose/ epoxy composites (Sturcova 2005). This is substantially higher than the shift rate reported herein. The stress transfer could have been affected by the aggregation of nanocellulose (i.e. reduction in the aspect ratio) fibrils within non-polar media due to insufficient surface esterification or possibly due to lower crystallinity of acetylated TOFC compared to tunicate.

The Raman band shifts with respect to strain exhibit similar trends as the representative stress-strain curves of the same composites show (Fig. 20).

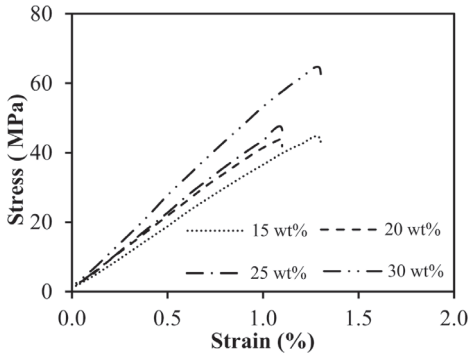

*Figure 20. Representative stress-strain curves of acetylated TOFC reinforced PLA composites with 15, 20, 25 and 30 wt% loads of the TOFC (adapted from **Paper V**).*

The composite containing 15 wt% load of TOFC had the lowest stiffness, which gradually increased upon the further addition of TOFC. The strain-to-failure was also higher for the composites with 15 and 30 wt% loads of TOFC (Fig. 20) as can

be also seen in Fig.19. This indicates that the Raman band shift clearly correlates with the mechanical properties of the composites.

The trend in shifting rates with respect to stress (**Paper IV**) was slightly different to the ones seen with respect to strain. The shift rate at lower weight fractions (15, 20, 25 %) virtually converged with the shifts in the pure cellulose film. The 30 wt% load composite exhibited different behaviour which was suggested by the higher shifting rate (27.9 cm^{-1}/GPa) compared to that of the pure cellulose film (16.6 cm^{-1}/GPa) (**Paper IV**). This supports the notion of good stress transfer through fibre-fibre and fibre-matrix interactions at 30 wt% load of TOFC compared to the other composites.

4.6 Structure of TOFC reinforced PLA and the effect of humidity on the mechanical properties

An investigation of the mechanical behaviour of composite films at elevated temperatures is important since thermoplastics are known for their poor performance at higher temperatures, especially over the T_g. An increase in storage modulus upon the addition of TOFC was observed using DMTA (Fig. 21).

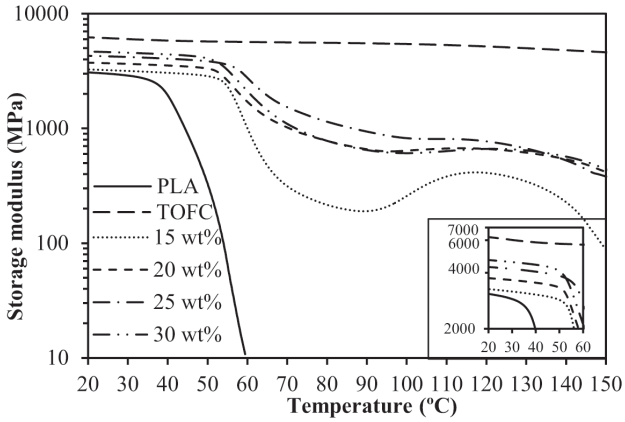

*Figure 21. Dependency of the storage modulus of the composites, with 15, 20, 25 and 30 wt% loads of TOFC, on temperature (**Paper V**).*

An increase in storage modulus correlated with the weight fraction of TOFC in the PLA matrix. The T_g, indicated by the abrupt drop in the storage modulus of PLA, was around 40 ºC whereas the composites mechanical properties remained virtually unchanged up to 60 ºC. However, the behaviour of PLA could also have been affected by residual solvent, inclusions, processing method or other side effects, thereby decreasing the softening temperature. Composites with 15 wt % load exhibited different mechanical behaviour compared to the other composites. Although the composite with 30 wt% load of TOFC had the highest modulus at 20 ºC it showed a higher decrease in the storage modulus at T_g compared to the 25 wt% load composite. This suggests higher chain mobility in composites with 30 wt% load, in turn implying a change in the prevailing interaction i.e. from fibril-matrix to fibril-fibril. Analogous findings were presented in **Paper IV**. Similar trends in the thermal-mechanical properties of cellulose reinforced composites have been reported previously (Suryanegara 2010; Suryanegara et al. 2009; Tingaut et al. 2010; Mathew et al 2005; Huda et al. 2005; Huda et al. 2006), however the crystallization behaviour observed in the present study was different.

Crystallization from a TOFC dispersion in PLA dissolved in chloroform was more pronounced than crystallization from the melt. This implies that alignment of polymer chains was hindered by the dense TOFC network. Although the composite with 15 wt% load exhibited cold crystallization which suggests that some polymer chains were able to align indicating that, probably, the percolation threshold is over 15 wt%. In fact, the highest crystallinity is achieved at 25 wt% load in both cases and decreases at 30 wt% load (**Paper V**). This corresponds to the notion of network formation at 30 wt % load as was mentioned in **Paper IV**. The greater crystallization from the dispersion could plausibly be attributed to lower viscosity and longer crystallization time compared to crystallization from the melt. It is worth noting that DSC cannot be directly compared to DMTA due to the different

natures of the techniques (Brown 2001). DSC is more suitable for evaluating T_g since it allows for the elimination of the effects of residual solvent, thermal history and other side effects on the structure of a polymer. Using DSC, it was found that T_g increased by approx. 8 % upon the addition of 25 wt% of TOFC. It can be seen in Fig.22 that composite with 15 wt% of TOFC had lower T_g compared to the pure PLA, most probably due to the absence of a network as has been mentioned.

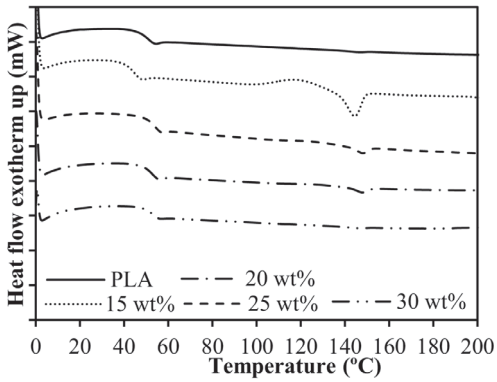

*Figure 22. DSC thermogram: 3rd stage - heating up to 200 ºC at 10 ºC/min of PLA film and TOFC/PLA composites with 15, 20, 25 and 30 wt% loads of TOFC (**Paper V**).*

Since cellulose is hydrophilic it is important to study how the addition of TOFC affects the mechanical behaviour of the composite in humid environment. The storage modulus at ~ 0 % RH was proportional to the weight fraction of TOFC (Fig. 23).

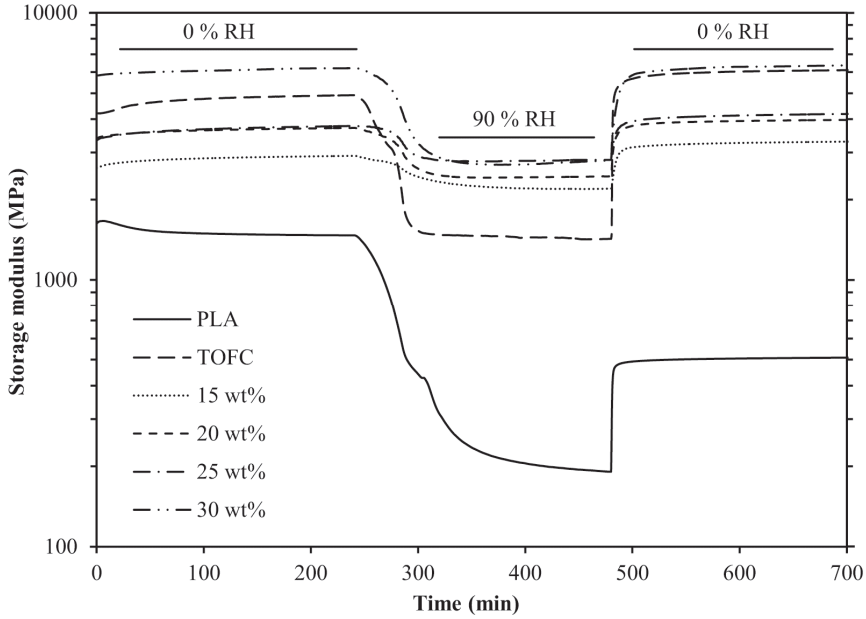

*Figure 23. Variation of the storage modulus of the composites with 15, 20, 25 and 30 wt% load of TOFC as well as of pure PLA and TOFC with respect to RH. The RH was cycled between 0 and 90 % at constant 30 ºC temperature (**Paper V**)*

The differences in the storage modulus diminished at 90 % RH. The pure TOFC film exhibited the greatest decline due to the well-known lubrication effect of water. For the same reason the storage modulus of the composite with 30 wt% load of TOFC exhibited slightly slower values than the composite with 25 wt% load. Nevertheless, the storage modulus recovered to values which are higher than the initial ones after one humidity cycle. This could result from the alignment of the nanofibrils in the moist environment (Peresin et al. 2010). Water facilitates slippage between fibrils without breakage since it forms hydrogen bonds with the cellulose. When water evaporates inter- and intra-fibrilar hydrogen bonds are recovered providing superior storage modulus.

5 CONCLUSIONS

The preparation method of the composite films plays a significant role in the mechanical behaviour of final material. Viscosity is an important factor affecting the dispersion and aggregation of cellulose nanofibrils. The effect of degassing is also closely related to viscosity, as removal of air at higher viscosities is limited. Thus the optimal parameters have to be chosen, depending on the weight fraction and morphology of the cellulose, to achieve the desired composite characteristics.

The deformation mechanisms in composites with low weight fractions of nanocellulose (< 10 wt%) are essentially different to the ones at higher weight fractions. Crazing, which is also DS dependent, is induced in MFC reinforced PLA composites leading to high strains-to-failure. A composite with 10 wt% load of MFC having a DS of 0.43 was toughened and strengthened suggesting a plausible practical implementation of these materials in the future. TOFC triggered crazing in a PLA matrix at lower weight fraction (1 wt%) compared to MFC, probably due to the higher surface area of TOFC. Crazing and consequently high strains-to-failure and toughness, could be result of several factors: i) fibril-fibril and fibril-matrix slippage; ii) introduced stiffness heterogeneity upon the addition of nanocellulose fibrils and iii) the introduction of voids, which act as non-bonded particles within the composite. Raman imaging was found to be a useful tool in studying the dispersion of cellulosic materials within a polymer matrix. Raman spectroscopy has shown that the percolation threshold of TOFC reinforced PLA composites is high and that network dominated deformation mechanisms take place at ~ 30 wt% load of TOFC. The thermal stability as well as the mechanical properties of the PLA matrix were significantly improved upon the addition of TOFC at 15, 20, 25 and 30 wt%. The properties of composites were also improved in humid environments.

Further studies in this field could concentrate on the effect of DS on the stress transfer mechanism in these composites as well as the effect of cellulose raw material on stress transfer and the toughening effect on polymer matrices. Additionally, the crystallization behaviour could be investigated with respect to DS, as it affects the surface energy of nanocellulose.

6 REFERENCES

Abdul Khalil, H.P.S., Bhat, A.H. & Ireana Yusra, A.F. 2012, "Green composites from sustainable cellulose nanofibrils: A review", *Carbohydrate Polymers,* vol. 87, no. 2, pp. 963-979.

Affdl, J.C.H. & Kardos, J.L. 1976, "The Halpin-Tsai equations: A review", *Polymer Engineering & Science,* vol. 16, no. 5, pp. 344-352.

Aharony, A. & Stauffer, D. 1994, *Introduction to percolation theory,* 2nd edn, Taylor & Francis, UK. 182 p.

Akhtar, W., Edwards, H.G.M., Farwell, D.W. & Nutbrown, M. 1997, "Fourier-transform Raman spectroscopic study of human hair", *Spectrochimica Acta Part A: Molecular and Biomolecular Spectroscopy,* vol. 53, no. 7, pp. 1021-1031.

Atalla, R.H., Whitmore, R.E. & Heimbach, C.J. 1980, "Raman Spectral Evidence for Molecular Orientation in Native Cellulosic Fibers", *Macromolecules,* vol. 13, no. 6, pp. 1717-1719.

Azizi Samir, M.A.S., Alloin, F. & Dufresne, A. 2005, "Review of Recent Research into Cellulosic Whiskers, Their Properties and Their Application in Nanocomposite Field", *Biomacromolecules,* vol. 6, no. 2, pp. 612-626.

Bakri, B. & Eichhorn, S.J. 2010, "Elastic coils: deformation micromechanics of coir and celery fibres", *Cellulose,* vol. 17, no. 1, pp. 1-11.

Batchelder, D.N. & Bloor, D. 1979, "Strain dependence of the vibrational modes of a diacetylene crystal", *Journal of Polymer Science: Polymer Physics Edition,* vol. 17, no. 4, pp. 569-581.

Blackwell, J., Vasko, P.D. & Koenig, J.L. 1970, "Infrared and Raman Spectra of the Cellulose from the Cell Wall of Valonia ventricosa", *Journal of Applied Physics,* vol. 41, no. 11, pp. 4375-4379.

Brown, M.E. 2001, *Introduction to Thermal Analysis: Techniques and Applications (2nd Edition),* Kluwer Academic Publishers, Secaucus, NJ, USA. 264 p.

Chakraborty, A., Sain, M. & Kortschot, M. 2006, "Reinforcing potential of wood pulp-derived microfibres in a PVA matrix", *Holzforschung,* vol. 60, no. 1, pp. 53-58.

Cheng, Q., Wang, S. & Harper, D.P. 2009, "Effects of process and source on elastic modulus of single cellulose fibrils evaluated by atomic force microscopy", *Composites Part A: Applied Science and Manufacturing,* vol. 40, no. 5, pp. 583-588.

Cheng, Q., Wang, S., Rials, T. & Lee, S. 2007, "Physical and mechanical properties of polyvinyl alcohol and polypropylene composite materials reinforced with fibril aggregates isolated from regenerated cellulose fibers", *Cellulose,* vol. 14, no. 6, pp. 593-602.

Cheng, Q., Wang, S. & Rials, T.G. 2009, "Poly(vinyl alcohol) nanocomposites reinforced with cellulose fibrils isolated by high intensity ultrasonication", *Composites Part A: Applied Science and Manufacturing,* vol. 40, no. 2, pp. 218-224.

Cooper, C.A. & Young, R.J. 1999, "Investigation of structure/property relationships in particulate composites through the use of Raman spectroscopy", *Journal of Raman Spectroscopy,* vol. 30, no. 10, pp. 929-938.

Cooper, C.A., Young, R.J. & Halsall, M. 2001, "Investigation into the deformation of carbon nanotubes and their composites through the use of Raman spectroscopy", *Composites Part A: Applied Science and Manufacturing,* vol. 32, no. 3-4, pp. 401-411.

Cox, H.L. 1952, "The elasticity and strength of paper and other fibrous materials", *British Journal of Applied Physics*, vol. 3, no. 3, pp. 72-79.

Davies, R.J., Montes-Moran, M.A., Riekel, C. & Young, R.J. 2001 "Single fibre deformation studies of poly(p-phenylene benzobisoxazole) fibres part I Determination of Crystal Modulus, *Journal of Materials Science,* vol. 36, no. 13, pp. 3079-3087

Davies, W.E.A. 1971a, "The theory of composite dielectrics", J*ournal of Physics D: Applied Physics,* vol. 4, no. 2, pp. 318-328

Davies, W.E.A. 1971b, "The elastic constants of a two-phase composite material", *Journal of Physics D: Applied Physics*, vol. 4, no. 8, pp. 1176-1181.

Duran, N., Lemes, A. P & Seabra, A.B. 2012, "Review of Cellulose Nanocrystals Patents: Preparation, Composites and General Applications", *Recent Patents on Nanotechnology*, vol. 6, no. 1, pp. 16-28

Edwards, H.G.M., Farwell, D.W. & Webster, D. 1997, "FT Raman microscopy of untreated natural plant fibres", *Spectrochimica Acta Part A: Molecular and Biomolecular Spectroscopy,* vol. 53, no. 13, pp. 2383-2392.

Eichhorn, S.J., Baillie, C.A., Zafeiropoulos, N., Mwaikambo, L.Y., Ansell, M.P., Dufresne, A., Entwistle, K.M., Herrera-Franco, P., Escamilla, G.C., Groom, L., Hughes, M., Hill, C., Rials, T.G. & Wild, P.M. 2001, "Review: Current international research into cellulosic fibres and composites", *Journal of Materials Science,* vol. 36, no. 9, pp. 2107-2131.

Eichhorn, S.J. & Davies, G.R. 2006, "Modelling the crystalline deformation of native and regenerated cellulose", *Cellulose,* vol. 13, no. 3, pp. 291-307.

Eichhorn, S.J., Dufresne, A., Aranguren, M., Marcovich, N.E., Capadona, J.R., Rowan, S.J., Weder, C., Thielemans, W., Roman, M., Renneckar, S., Gindl, W., Veigel, S., Keckes, J., Yano, H., Abe, K., Nogi, M., Nakagaito, A.N., Mangalam, A., Simonsen, J. & Benight, A.S. 2010, "Review: current international research into cellulose nanofibres and nanocomposites", *Journal of Materials Science,* vol. 45, no. 1, pp. 1-33.

Eichhorn, S.J., Hughes, M., Snell, R. & Mott, L. 2000, "Strain induced shifts in the Raman spectra of natural cellulose fibers", *Journal of Materials Science Letters,* vol. 19, no. 8, pp. 721-723.

Eichhorn, S.J., Sirichaisit, J. & Young, R.J. 2001, "Deformation mechanisms in cellulose fibres, paper and wood", *Journal of Materials Science,* vol. 36, no. 13, pp. 3129-3135.

Eichhorn, S.J. & Young, R.J. 2001, "The Young's modulus of a microcrystalline cellulose", *Cellulose,* vol. 8, no. 3, pp. 197-207.

Eichhorn, S.J., Young, R.J. 2004, "Composite micromechanics of hemp fibres and epoxy resin microdroplets", *Composites Science and Technology,* vol. 64, pp. 767-772.

Eichhorn, S.J., Young, R.J. & Yeh, W.Y. 2001, "Deformation Processes in Regenerated Cellulose Fibers", *Textile Research Journal,* vol. 71, no. 2, pp. 121-129.

EPA - US Environmental Protection Agency 2010, "Municipal Solid Waste Generation, Recycling, and Disposal in the United States: Facts and Figures for 2009", 12 p. [online]. Available from: http://www.epa.gov/epawaste/nonhaz/municipal/pubs/msw2009-fs.pdf

Favier, V., Cavaille, J.Y., Canova, G.R. & Shrivastava, S.C. 1997, "Mechanical percolation in cellulose whisker nanocomposites", *Polymer Engineering & Science,* vol. 37, no. 10, pp. 1732-1739.

Favier, V., Chanzy, H. & Cavaille, J.Y. 1995, "Polymer Nanocomposites Reinforced by Cellulose Whiskers", *Macromolecules,* vol. 28, no. 18, pp. 6365-6367.

Fugetsu, B., Sano, E., Sunada, M., Sambongi, Y., Shibuya, T., Wang, X. & Hiraki, T. 2008, "Electrical conductivity and electromagnetic interference shielding efficiency of carbon nanotube/cellulose composite paper", *Carbon,* vol. 46, no. 9, pp. 1256-1258.

Gabr, M.H., Elrahman, M.A., Okubo, K. & Fujii, T. 2010a, "Effect of microfibrillated cellulose on mechanical properties of plain-woven CFRP reinforced epoxy", *Composite Structures,* vol. 92, no. 9, pp. 1999-2006.

Gabr, M.H., Elrahman, M.A., Okubo, K. & Fujii, T. 2010b, "A study on mechanical properties of bacterial cellulose/epoxy reinforced by plain woven carbon fiber modified with liquid rubber", *Composites Part A: Applied Science and Manufacturing,* vol. 41, no. 9, pp. 1263-1271.

Gabr, M., Elrahman, M., Okubo, K. & Fujii, T. 2010c, "Interfacial adhesion improvement of plain woven carbon fiber reinforced epoxy filled with micro-fibrillated cellulose by addition liquid rubber", *Journal of Materials Science,* vol. 45, no. 14, pp. 3841-3850.

Garcia, R., Thielemans, W. & Dufresne, A. 2006, "Sisal cellulose whiskers reinforced polyvinyl acetate nanocomposites", *Cellulose,* vol. 13, no. 3, pp. 261-270.

Gierlinger, N. & Schwanninger, M. 2007, "The potential of Raman microscopy and Raman imaging in plant research", *Spectroscopy,* vol. 21, no. 2, pp. 69-89.

Gierlinger, N., Schwanninger, M., Reinecke, A. & Burgert, I. 2006, "Molecular Changes during Tensile Deformation of Single Wood Fibers Followed by Raman Microscopy", *Biomacromolecules,* vol. 7, no. 7, pp. 2077-2081.

Henriksson, M., Berglund, L.A., Isaksson, P., Lindström, T. & Nishino, T. 2008, "Cellulose Nanopaper Structures of High Toughness", *Biomacromolecules,* vol. 9, no. 6, pp. 1579-1585.

Heux, L., Chauve, G. & Bonini, C. 2000, "Nonflocculating and Chiral-Nematic Self-ordering of Cellulose Microcrystals Suspensions in Nonpolar Solvents", *Langmuir,* vol. 16, no. 21, pp. 8210-8212.

Hill, R. 1964, "Theory of mechanical properties of fibre-strengthened materials: II. Inelastic behaviour", *Journal of the Mechanics and Physics of Solids,* vol. 12, no. 4, pp. 213-218.

Hill, R. 1963, "Elastic properties of reinforced solids: Some theoretical principles", *Journal of the Mechanics and Physics of Solids,* vol. 11, no. 5, pp. 357-372.

Hinterstoisser, B., Åkerholm, M. & Salmen, L. 2003, "Load Distribution in Native Cellulose", *Biomacromolecules,* vol. 4, no. 5, pp. 1232-1237.

Hogg, L.J., Edwards, H.G.M., Farwell, D.W. & Peters, A.T. 1994, "FT Raman spectroscopic studies of wool", *Journal of the Society of Dyers and Colourists,* vol. 110, no. 5-6, pp. 196-199.

Huda, M.S., Drzal, L.T., Misra, M. & Mohanty, A.K. 2006, "Wood-fiber-reinforced poly(lactic acid) composites: Evaluation of the physicomechanical and morphological properties", *Journal of Applied Polymer Science,* vol. 102, no. 5, pp. 4856-4869.

Huda, M.S., Mohanty, A.K., Drzal, L.T., Schut, E. & Misra, M. 2005, ""Green" composites from recycled cellulose and poly(lactic acid): Physico-mechanical and morphological properties evaluation", *Journal of Materials Science,* vol. 40, no. 16, pp. 4221-4229.

Hull, D. & Clyne, T.W. 1996, "An Introduction to Composite Materials", 2nd edn, *Cambridge University Press*, Cambridge. 326 p.

I'Anson, S.J. & Sampson, W.W. 2007, "Competing Weibull and stress-transfer influences on the specific tensile strength of a bonded fibrous network", *Composites Science and Technology,* vol. 67, no. 7-8, pp. 1650-1658.

Iwamoto, S., Kai, W., Isogai, A. & Iwata, T. 2009, "Elastic Modulus of Single Cellulose Microfibrils from Tunicate Measured by Atomic Force Microscopy", *Biomacromolecules,* vol. 10, no. 9, pp. 2571-2576.

Jonoobi, M., Harun, J., Mathew, A.P. & Oksman, K. 2010a, "Mechanical properties of cellulose nanofiber (CNF) reinforced polylactic acid (PLA) prepared by twin screw extrusion", *Composites Science and Technology,* vol. 70, no. 12, pp. 1742-1747.

Jonoobi, M., Harun, J., Mathew, A., Hussein, M. & Oksman, K. 2010b, "Preparation of cellulose nanofibers with hydrophobic surface characteristics", *Cellulose,* vol. 17, no. 2, pp. 299-307.

Klemm, D., Philipp, B., Heinze, T., Heinze, U. & Wagenknecht, W. 1998, "General Considerations on Structure and Reactivity of Cellulose: Section 2.1-2.1.4" in *Comprehensive Cellulose Chemistry* Wiley-VCH Verlag GmbH & Co. KGaA, , pp. 9-29.

Korhonen, J.T., Hiekkataipale, P., Malm, J., Karppinen, M., Ikkala, O. & Ras, R.H.A. 2011, "Inorganic Hollow Nanotube Aerogels by Atomic Layer Deposition onto Native Nanocellulose Templates", *ACS Nano,* vol. 5, no. 3, pp. 1967-1974.

Kvien, I., Tanem, B.S. & Oksman, K. 2005, "Characterization of Cellulose Whiskers and Their Nanocomposites by Atomic Force and Electron Microscopy", *Biomacromolecules,* vol. 6, no. 6, pp. 3160-3165.

Lin, N., Huang, J., Chang, P.R., Feng, J. & Yu, J. 2011, "Surface acetylation of cellulose nanocrystal and its reinforcing function in poly(lactic acid)", *Carbohydrate Polymers,* vol. 83, no. 4, pp. 1834-1842.

Liu, A., Walther, A., Ikkala, O., Belova, L. & Berglund, L.A. 2011, "Clay Nanopaper with Tough Cellulose Nanofiber Matrix for Fire Retardancy and Gas Barrier Functions", *Biomacromolecules,* vol. 12, no. 3, pp. 633-641.

Ljungberg, N., Bonini, C., Bortolussi, F., Boisson, C., Heux, L. & Cavaillé, J.Y. 2005, "New Nanocomposite Materials Reinforced with Cellulose Whiskers in Atactic Polypropylene: Effect of Surface and Dispersion Characteristics", *Biomacromolecules,* vol. 6, no. 5, pp. 2732-2739.

Lu, J., Wang, T. & Drzal, L.T. 2008, "Preparation and properties of microfibrillated cellulose polyvinyl alcohol composite materials", *Composites Part A: Applied Science and Manufacturing,* vol. 39, no. 5, pp. 738-746.

Mangalam, A.P., Simonsen, J. & Benight, A.S. 2009, "Cellulose/DNA Hybrid Nanomaterials", *Biomacromolecules,* vol. 10, no. 3, pp. 497-504.

Marks, K. & Howden, D. 2008, "The world's rubbish dump: a tip that stretches from Hawaii to Japan".*The Independent.* [online] Available from: http://www.independent.co.uk/environment/green-living/the-worlds-rubbish-dump-a-tip-that-stretches-from-hawaii-to-japan-778016.html

Mathew, A.P., Oksman, K. & Sain, M. 2005, "Mechanical properties of biodegradable composites from poly lactic acid (PLA) and microcrystalline cellulose (MCC)", *Journal of Applied Polymer Science,* vol. 97, no. 5, pp. 2014-2025.

Meyers, M.A., Chen, P., Lin, A.Y. & Seki, Y. 2008, "Biological materials: Structure and mechanical properties", *Progress in Materials Science,* vol. 53, no. 1, pp. 1-206.

Mitra, V.K., William M. Risen, J. & Baughman, R.H. 1977, "A laser Raman study of the stress dependence of vibrational frequencies of a monocrystalline polydiacetylene", *The Journal of chemical physics,* vol. 66, no. 6, pp. 2731-2736.

Moon, R.J., Martini, A., Nairn, J., Simonsen, J. & Youngblood, J. 2011, "Cellulose nanomaterials review: structure, properties and nanocomposites", *Chemical Society Reviews,* vol. 40, no. 7, pp. 3941-3994.

Nakagaito, A.N., Fujimura, A., Sakai, T., Hama, Y. & Yano, H. 2009, "Production of microfibrillated cellulose (MFC)-reinforced polylactic acid (PLA) nanocomposites from sheets obtained by a papermaking-like process", *Composites Science and Technology,* vol. 69, no. 7-8, pp. 1293-1297.

Okahisa, Y., Yoshida, A., Miyaguchi, S. & Yano, H. 2009, "Optically transparent wood–cellulose nanocomposite as a base substrate for flexible organic light-emitting diode displays", *Composites Science and Technology,* vol. 69, no. 11-12, pp. 1958-1961.

Oksman, K., Mathew, A.P., Bondeson, D. & Kvien, I. 2006, "Manufacturing process of cellulose whiskers/polylactic acid nanocomposites", *Composites Science and Technology,* vol. 66, no. 15, pp. 2776-2784.

Okubo, K., Fuji, T. & Yamashita, N. 2005, "Improvement of Interfacial Adhesion in Bamboo Polymer Composite Enhanced with Micro-Fibrillated Cellulose", *JSME International Journal Series A Solid Mechanics and Material Engineering,* vol. 48, no. 4, pp. 199-204.

Okubo, K., Fujii, T. & Thostenson, E.T. 2009, "Multi-scale hybrid biocomposite: Processing and mechanical characterization of bamboo fiber reinforced PLA with microfibrillated cellulose", *Composites Part A: Applied Science and Manufacturing,* vol. 40, no. 4, pp. 469-475.

Olsson, R., Azizi Samir, M.A.S., Salazar-Alvarez, G., Belova, L., Strom, V., Berglund, L.A., Ikkala, O., Nogues, J. & Gedde, U.W. 2010, "Making flexible magnetic aerogels and stiff magnetic nanopaper using cellulose nanofibrils as templates", *Nature Nanotechnology,* vol. 5, no. 8, pp. 584-588.

O'Sullivan, A. 1997, "Cellulose: the structure slowly unravels", *Cellulose,* vol. 4, no. 3, pp. 173-207.

Ouali, N., Cavaille, J.Y. & Perez, J. 1991, "Elastic, Viscoelastic and Plastic Behavior of Multiphase Polymer Blends", *Plastics, Rubber and Composites Processing and Applications,* vol. 16, no. 1, pp. 55-60.

Peetla, P., Schenzel, K.C. & Diepenbrock, W. 2006, "Determination of Mechanical Strength Properties of Hemp Fibers Using Near-Infrared Fourier Transform Raman Microspectroscopy", *Applied Spectroscopy,* vol. 60, no. 6, pp. 682-691.

Pei, A., Zhou, Q. & Berglund, L.A. 2010, "Functionalized cellulose nanocrystals as biobased nucleation agents in poly(l-lactide) (PLLA) - Crystallization and mechanical property effects", *Composites Science and Technology,* vol. 70, no. 5, pp. 815-821.

PEMRG Plastics Europe market research group 2010, " Plastics – the facts 2010. An analysis of European plastics production, demand and recovery for 2009", [Online] Available from: http://www.plasticseurope.org/documents/document/20101028135906-final_plasticsthefacts_26102010_lr.pdf.

Peresin, M.S., Habibi, Y., Vesterinen, A., Rojas, O.J., Pawlak, J.J. & Seppälä, J.V. 2010, "Effect of Moisture on Electrospun Nanofiber Composites of Poly(vinyl alcohol) and Cellulose Nanocrystals", *Biomacromolecules,* vol. 11, no. 9, pp. 2471-2477.

Postek, M.T., Vladár, A., Dagata, J., Farkas, N., Ming, B., Wagner, R., Raman, A., Moon, R.J., Sabo, R., Wegner, T.H. & Beecher, J. 2011, "Development of the metrology and imaging of cellulose nanocrystals", *Measurement Science and Technology,* vol. 22, no. 2, pp. 024005.

Pullawan, T., Wilkinson, A.N. & Eichhorn, S.J. 2010, "Discrimination of matrix-fibre interactions in all-cellulose nanocomposites", *Composites Science and Technology,* vol. 70, no. 16, pp. 2325-2330.

Quan, H., Li, Z., Yang, M. & Huang, R. 2005, "On transcrystallinity in semi-crystalline polymer composites", *Composites Science and Technology,* vol. 65, no. 7–8, pp. 999-1021.

Quero, F., Nogi, M., Yano, H., Abdulsalami, K., Holmes, S.M., Sakakini, B.H. & Eichhorn, S.J. 2010, "Optimization of the Mechanical Performance of Bacterial Cellulose/Poly(l-lactic) Acid Composites", *ACS Applied Materials & Interfaces,* vol. 2, no. 1, pp. 321-330.

Quesada Cabrera, R., Meersman, F., McMillan, P.F. & Dmitriev, V. 2011, "Nanomechanical and Structural Properties of Native Cellulose Under Compressive Stress", *Biomacromolecules,* vol. 12, no. 6, pp. 2178-2183.

Raman, C.V. & Krishnan, K.S. 1928, "A New Type of Secondary Radiation", *Nature,* vol. 121, pp. 501-502.

Ranby, B.G. 1951, "Fibrous macromolecular systems. Cellulose and muscle. The colloidal properties of cellulose micelles", *Discussions of the Faraday Society,* vol. 11, pp. 158-164.

Roohani, M., Habibi, Y., Belgacem, N.M., Ebrahim, G., Karimi, A.N. & Dufresne, A. 2008, "Cellulose whiskers reinforced polyvinyl alcohol copolymers nanocomposites", *European Polymer Journal,* vol. 44, no. 8, pp. 2489-2498.

Rusli, R., Shanmuganathan, K., Rowan, S.J., Weder, C. & Eichhorn, S.J. 2011, "Stress Transfer in Cellulose Nanowhisker Composites: Influence of Whisker Aspect Ratio and Surface Charge", *Biomacromolecules,* vol. 12, no. 4, pp. 1363-1369.

Rusli, R., Shanmuganathan, K., Rowan, S.J., Weder, C. & Eichhorn, S.J. 2010, "Stress-Transfer in Anisotropic and Environmentally Adaptive Cellulose Whisker Nanocomposites", *Biomacromolecules,* vol. 11, no. 3, pp. 762-768.

Saito, T., Nishiyama, Y., Putaux, J., Vignon, M. & Isogai, A. 2006, "Homogeneous Suspensions of Individualized Microfibrils from TEMPO-Catalyzed Oxidation of Native Cellulose", *Biomacromolecules,* vol. 7, no. 6, pp. 1687-1691.

Santiago C.M., Johnson, G. & French, A. 2011, "Young's modulus calculations for cellulose I_β by MM3 and quantum mechanics", *Cellulose,* vol. 18, no. 3, pp. 505-516.

Shyng, Y., Bennett, J., Young, R., Davies, R. & Eichhorn, S. 2006, "Analysis of interfacial micromechanics of model composites using synchrotron microfocus X-ray diffraction", *Journal of Materials Science,* vol. 41, no. 20, pp. 6813-6821.

Siro, I. & Plackett, D. 2010, "Microfibrillated cellulose and new nanocomposite materials: a review", *Cellulose,* vol. 17, no. 3, pp. 459-494.

Smith, E. & Geoffrey, D. 2005, "Modern Raman Spectroscopy: A Practical Approach"*, John Wiley & Sons*, Chichester, England. 210 p.

Stevens, E.S. 2001, "Green plastics: An introduction to the new science of biodegradable plastics"*, Princeton University Press*, Princeton, New Jersey, USA. 272 p.

Sturcova, A. 2005, "Elastic modulus and stress-transfer properties of tunicate cellulose whiskers", *Biomacromolecules,* vol. 6, no. 2, pp. 1055-1061.

Suryanegara, L. 2010, "Thermo-mechanical properties of microfibrillated cellulose-reinforced partially crystallized PLA composites", *Cellulose,* vol. 17, no. 4, pp. 771-778.

Suryanegara, L., Nakagaito, A.N. & Yano, H. 2009, "The effect of crystallization of PLA on the thermal and mechanical properties of microfibrillated cellulose-reinforced PLA composites", *Composites Science and Technology,* vol. 69, no. 7-8, pp. 1187-1192.

Takayanagi, M., Imada, K. & Kajiyama, T. 1967, "Mechanical properties and fine structure of drawn polymers", *Journal of Polymer Science Part C: Polymer Symposia,* vol. 15, no. 1, pp. 263-281.

Tanaka, F. & Iwata, T. 2006, "Estimation of the Elastic Modulus of Cellulose Crystal by Molecular Mechanics Simulation", *Cellulose,* vol. 13, no. 5, pp. 509-517.

Tashiro, K. & Kobayashi, M. 1985, "Calculation of crystallite modulus of native cellulose", *Polymer Bulletin*, vol. 14, no. 3-4, pp. 213-218.

Tingaut, P., Zimmermann, T. & Lopez-Suevos, F. 2010, "Synthesis and Characterization of Bionanocomposites with Tunable Properties from Poly(lactic acid) and Acetylated Microfibrillated Cellulose", *Biomacromolecules,* vol. 11, no. 2, pp. 454-464.

Tome, L.C., Pinto, R.J.B., Trovatti, E., Freire, C.S.R., Silvestre, A.J.D., Neto, C.P. & Gandini, A. 2011, "Transparent bionanocomposites with improved properties prepared from acetylated bacterial cellulose and poly(lactic acid) through a simple approach", *Green Chemistry,* vol. 13, no. 2, pp. 419-427.

Treloar, L.R.G. 1941, "Crystallisation phenomena in raw rubber", *Transactions of the Faraday Society,* vol. 37, pp. 84-97.

Turbak, A.F., Snyder, F.W. & Sandberg, K.R. 1983, "Microfibrillated cellulose, a new cellulose product: properties, uses, and commercial potential", *J.Appl.Polym.Sci.: Appl.Polym.Symp.,* vol. 37, pp. 815.

Veigel, S., Müller, U., Keckes, J., Gindl-Altmutter, W. 2011, "Cellulose nanofibrils as filler for adhesives: Effect on specific fracture energy of solid wood-adhesive bonds. *Cellulose,* vol. 18, no. 5, pp. 1227-1237.

Ward, I.M. 1962, "Optical and Mechanical Anisotropy in Crystalline Polymers", *Proceedings of the Physical Society,* vol. 80, no. 5, pp. 1176-1188.

Weibull, W. 1951, "A Statistical Distribution Function of Wide Applicability", *Journal of Applied Mechanics-Transactions of the Asme,* vol. 18, no. 3, pp. 293-297.

Wiley, J.H. & Atalla, R.H. 1987, "Band assignments in the raman spectra of celluloses", *Carbohydrate research,* vol. 160, pp. 113-129.

Yano, H., Sugiyama, J., Nakagaito, A.N., Nogi, M., Matsuura, T., Hikita, M. & Handa, K. 2005, "Optically Transparent Composites Reinforced with Networks of Bacterial Nanofibers", *Advanced Materials,* vol. 17, no. 2, pp. 153-155.

Yoon, S.H., Jin, H., Kook, M. & Pyun, Y.R. 2006, "Electrically Conductive Bacterial Cellulose by Incorporation of Carbon Nanotubes", *Biomacromolecules,* vol. 7, no. 4, pp. 1280-1284.

Young, R.J. & Lovell, P.A. 1991, "Introduction to polymers", 2nd edn, *Chapman & Hall*, Cambridge. 443 p.

Young, R.J., Day, R.J. & Zakikhani, M. 1990, "The structure and deformation behaviour of poly(*p*-phenylene benzobisoxazole) fibres", *Journal of Materials Science,* vol. 25, no. 1, pp. 127-136.

Young, R.J. & Eichhorn, S.J. 2007, "Deformation Mechanisms in Polymer Fibres and Nanocomposites ", *Polymer,* vol. 48, no. 1, pp. 2-18.

Yousefi, H., Nishino, T., Faezipour, M., Ebrahimi, G. & Shakeri, A. 2011, "Direct Fabrication of all-Cellulose Nanocomposite from Cellulose Microfibers Using Ionic Liquid-Based Nanowelding", *Biomacromolecules,* vol. 12, no. 11, pp. 4080-4085.

Zimmermann, T., Pöhler, E. & Geiger, T. 2004, "Cellulose Fibrils for Polymer Reinforcement", *Advanced Engineering Materials,* vol. 6, no. 9, pp. 754-761.

Aalto-DD 109/2012

ISBN 978-952-60-4749-2
ISBN 978-952-60-4750-8 (pdf)
ISSN-L 1799-4934
ISSN 1799-4934
ISSN 1799-4942 (pdf)

Aalto University
School of Chemical Technology
Department of Forest Products Technology
www.aalto.fi

BUSINESS +
ECONOMY

ART +
DESIGN +
ARCHITECTURE

SCIENCE +
TECHNOLOGY

CROSSOVER

**DOCTORAL
DISSERTATIONS**